Small-Scale Smart Grid Construction and Analysis

By

Nicholas James Surface

Submitted to the graduate degree program in Mechanical Engineering and the Graduate Faculty of the University of Kansas in partial fulfillment of the requirements for the degree of Master of Science.

_____

Chairperson Dr. C. Depcik

_____

Dr. R. Dougherty

_____

Dr. T. Faddis

Date Defended: 18 April 2014

The Thesis Committee for Nicholas James Surface
certifies that this is the approved version of the following thesis:

Small-Scale Smart Grid Construction and Analysis

_____
Chairperson Dr. C. Depcik

Date approved: 22 April 2014

Abstract

The smart grid (SG) is a commonly used catch-phrase in the energy industry yet there is no universally accepted definition. The objectives and most useful concepts have been investigated extensively in economic, environmental and engineering research by applying statistical knowledge and established theories to develop simulations without constructing physical models. In this study, a small-scale version (SSSG) is constructed to physically represent these ideas so they can be evaluated. Results of construction show data acquisition three times more expensive than the grid itself although mainly due to the incapability to downsize 70% of data acquisition costs to small-scale. Experimentation on the fully assembled grid exposes the limitations of low cost modified sine wave power, significant enough to recommend pure sine wave investment in future SSSG iterations. Findings can be projected to full-size SG at a ratio of 1:10, based on the appliance representing average US household peak daily load. However this exposes disproportionalities in the SSSG compared with previous SG investigations and recommended changes for future iterations are established to remedy this issue. Also discussed are other ideas investigated in the literature and their suitability for SSSG incorporation. It is highly recommended to develop a user-friendly bidirectional charger to more accurately represent vehicle-to-grid (V2G) infrastructure. Smart homes, BEV swap stations and pumped hydroelectric storage can also be researched on future iterations of the SSSG.

Acknowledgements

First and foremost, I would especially like to thank to Dr. Chris Depcik for establishing the Ecohawks and this project, and your tremendous support, knowledge, advice and time over the last four years.

I also wish to thank my entire team at the Ecohawks especially Bryan Strecker, Mickey Clemen and Jon Mattson for their equal contribution to planning and assembling the SSSG in time and under budget for the EPA P3 competition in Washington DC.

Thanks to the EPA for providing the initial and most significant financial backing to the project. Also to National Instruments Corp. for providing a 60% discount on all data acquisition modules and free LabVIEW training.

I would finally like to thank the University of Kansas Mechanical Engineering Department for providing facilities, support and invaluable advice, including the professors, technicians and support staff.

Table of contents

Abstract ..... **iii**
Acknowledgements ..... **iv**
Table of contents ..... **v**
List of figures ..... **vii**
List of tables ..... **ix**
Acronyms ..... **x**
1. Introducing the Smart Grid **1**
1.1 Introducing key SG features and concepts 2
1.2. Smart energy markets - dynamic pricing and prosumer communities 5
1.3. SG experimentation 6
2. Small-Scale Smart Grid (SSSG) Planning and Design **8**
2.1. SSSG Proposition 8
2.2. SSSG Architecture 9
2.3. LV Programming 14
3. SSSG Results - Construction and Experiments **22**
3.1 Construction results including amendments from initial design 22
3.1.1. Smart grid assembly 23
3.1.2. Data acquisition and sensors 27
3.2 Experimental results 30
4. Discussion of SSSG Results **37**
4.1 Projecting SSSG results to full-size SG 37
4.1.1 Test #1 discussion 37
4.1.2 Test #2 discussion 38
4.1.3 Test #3 discussion 39
4.1.4 Test #4 discussion 40
4.1.5 Test #5 discussion 41
4.2 Other SG developments 42
4.2.1 Other renewable and carbon-neutral power generation 42
4.2.2 Improved BEV technology 45
4.2.3 Bidirectional V2G infrastructure 47
4.2.4 BEV battery swap stations 48

4.2.5 Smart homes/buildings 48
4.2.6 Economic, social, and policy hurdles 49
4.3 Future SSSG summary 51
5. Conclusion **53**
References **55**

List of figures

Figure 1. Share of energy consumed by major sectors of the economy, 2010 2

Figure 2. Classification of electric vehicle (EV) types....3

Figure 3. Functional model of SSSG concept 9

Figure 4. Diagram of SSSG cart....13

Figure 5. Screenshot of front panel of the SSSG....14

Figure 6. Screenshot of PV panel and appliance (POP) sub-VIs....15

Figure 7. LV program code hierarchy indicating links between VIs 15

Figure 8. MainFlowChartDisplay.vi code 16

Figure 9. ChargingDisplays.vi code 17

Figure 10. DischargingDisplays.vi code....17

Figure 11. LABs and Cobras.vi code....18

Figure 12. Gen and Sinks.vi code....19

Figure 13. SelectColor.vi code 19

Figure 14. WeatherReadings.vi code 20

Figure 15. AC Voltages.vi code 20

Figure 16. Charging Phase Readings RT.vi code....21

Figure 17. Full SSSG cart assembly presented at EPA P3 competition in Washington DC 22

Figure 18. From left to right PV panels: (a) in-house 24VDC and (b) HQRP mono-crystalline 20.7VDC 24

Figure 19. From left to right: Optima Lead Acid Battery (BlueLAB), Xantrex C35 Charge Controller (XCC), and Venom Pro Charger (VPC) 25

Figure 20. From left to right: A123 $LiFePO_4$ cells (LIB) and Elithion Lithiumate Pro (BMS) 25

Figure 21. From left to right inverters: Cobra 400W (INV1), Cobra 800W (INV2) and AIMS 600W (INV3)....26

Figure 22. SG diagram with average power flows and efficiencies corresponding to test #1....31

Figure 23. Power drawn by the popcorn maker over four cycles....32

Figure 24. Power flow from LAB to POP with the top figure indicating INV1 to POP and the bottom figure

demonstrating LAB1 to INV1 33

Figure 25. Power flow from LIB to INV1 to POP 34

Figure 26. Power flow from PV to XCC to LAB in clear conditions 35

Figure 27. Power flow from PV to XCC to LAB in changing overcast conditions 35

Figure 28. Ferrite bead tested on the SSSG 38

Figure 29. Renewable share of US electricity production 1980-2011 43

Figure 30. Carbon-neutral share of US electricity production 1980-2011 43

Figure 31. Hydroelectric bidirectional generator/pump design for energy storage. Clockwise from top left: housing, impeller, vane pump assembly (x2) 45

Figure 32. Future SSSG block diagram 51

List of tables

Table 1. Components and their functions 10

Table 2. Planned expenditures for the SSSG 11

Table 3. Final expenditures 23

Table 4. CRIO slots and module channel assignments 28

Table 5. Common battery chemistries and their attributes 41

Table 6. Theoretical and practical energy densities of various chemistries [52] 46

Acronyms

AC	Alternating current
AER	All-electric range
BESS	Battery energy storage system
BEV	Battery electric vehicle
BLUE Map	IEA “best case scenario” targets for cutting CO_2 emissions by 2050
BMS	Battery management system
C-rate	Normalized battery discharge current
CCCV	Constant current, constant voltage charger
CEER	Council of European Energy Regulators
CNS	Carbon-neutral energy sources
CRIO	NI LV compact reconfigurable I/O chassis
DC	Direct current
DoE	US Department of Energy
DPDT	Double pole double throw
EPA	US Environmental Protection Agency
EPRI	Electric Power Research Institute
EV	Electric vehicle
G2V	Grid-to-vehicle
GDP	Gross domestic product
GEN	Gasoline generator or conventional grid outlet
GEV	Grid electric vehicle
GHG	Greenhouse gases
GSHP	Ground source heat pump
HEV	Hybrid electric vehicle
HQRP	High Quality Reasonable Price Corporation
I/O	Input/output

ICE	Internal combustion engine
ICT	Information and communication technology
IEA	International Energy Agency
INV	Inverter
INV1	400W Cobra MSW inverter
INV2	800W Cobra MSW inverter
INV3	600W AIMS PSW inverter
LAB	Lead acid battery bank
LAB1	Optima Blue Top LAB
LAB2	AAE Marine LAB
LEM	Liaisons Electroniques-Mécaniques Corp. current sensor
LIB	Lithium-ion battery
LV	NI LabVIEW
MSW	Modified sine wave
NI	National Instruments Corporation
NI-9201	NI 8-channel 10V sensor module
NI-9211	NI 4-channel 80mV sensor module
NI-9221	NI 8-channel 60V sensor module
NI-9225	NI 3-channel 300V sensor module
NI-9227	NI 4-channel 5A sensor module
NI-9401	NI 8-channel digital I/O module
OECD	Organization for Economic Co-operation and Development
PC	Personal computer
PHEV	Plug-in hybrid electric vehicle
POP	Popcorn maker
PSW	Pure sine wave
PV	Photovoltaic

RE	Renewable energy
RES	Renewable energy sources
REV	Range-extended hybrid electric vehicle
RMS	Root mean square
RT	Real-time
SAE	Society of automotive engineers
SC	Solar collector
SG	Smart grid
SOC	Battery state-of-charge
SPDT	Single pole double throw
SSSG	Small-scale smart grid
T&D	Transmission and distribution
TDMS	LV technical data management solution
V2G	Vehicle-to-grid
V2H	Vehicle-to-home
V2V	Vehicle-to-vehicle
VI	LV virtual instrument
VPC	Venom Pro Charger
WT	Wind turbine
XCC	Xantrex charge controller

1. Introducing the Smart Grid

Political demand for lower reliance on unsustainable fossil fuels and reduction of greenhouse gas (GHG) emissions has put pressure on the energy industry to become more efficient, while maintaining reliability of service [1]. As a result, the energy market has undergone fundamental changes in recent years, including the strong growth of decentralized energy generation including greater reliance on renewable energy sources (RES). In essence, the energy industry is endeavoring to do more with less and create a smarter connectivity between conventional and alternative power sources.

The term “smart grid” (SG) is one of the most commonly used catch-phrases in the energy industry and its concept continues to evolve with developments in various technologies producing lower costs and higher availability. Although a precise definition does not, and probably cannot exist, several pseudo-official definitions have been generated [2]. For example, the Council of European Energy Regulators (CEER) defines SG objectives in terms of improving capacity, flexibility, renewable energy (RE) integration, new storage technologies, and more active demand-side response [3]. The US Department of Energy (DoE), on the other hand, has no comprehensive definition but summarizes its vision of making the grid “smarter” by [4]:

- Deploying advanced devices that give real-time (RT) data on system conditions
- Supporting two-way flow of electricity and information between utility and users
- Enabling demand response, outage management and other important capabilities

The overall consensus regarding the usefulness of SGs can be summarized as [2]:

- Integrating RES and energy storage while optimizing their contribution
- Integrating electric vehicles through smart bidirectional charging strategies
- Introducing consumers as more active players in the system
- Promoting innovative new energy products and services related to load handling
- Deploying “smart” agents for greater automation concerning grid operations including optimization
- Enhancing the quality of power supply (fewer outages)

- Anticipating outages with necessary upgrading or maintenance of self-adapting networks
- Developing information and communication technology (ICT) including data storage and management

While SGs have been extensively studied, practical models have not been constructed. Instead, theoretical models have been simulated, such as a direct current (DC) smart home in which a photovoltaic (PV) source was used to power a battery and heat pump [5]. This example demonstrates one of the key issues with integrating RES into the conventional grid; the mismatch between supply and demand. Often, solar and wind RES are not available during the time that they would be needed (e.g., wind at night when grid demand is low). Proper integration of RES through smoothing the volatile peaks and troughs of both generation and consumption is one of the most useful features of the SG, known in the business as peak shaving and valley filling. Several studies have already addressed the issue of utilizing excess RE, both solar and wind, through various schemes [6, 7]. This study will attempt to analyze the full energy cycle from generation to storage to consumption by constructing an entire SG model.

1.1 Introducing key SG features and concepts

Having established the objectives of the SG, specific ideas and solutions can be developed. Many of these ideas are not particularly new or innovative but are receiving attention today thanks to modern advances in various technologies, most notably information and communication technology (ICT); however, others remain limited by modern battery technology and consumer attitudes.

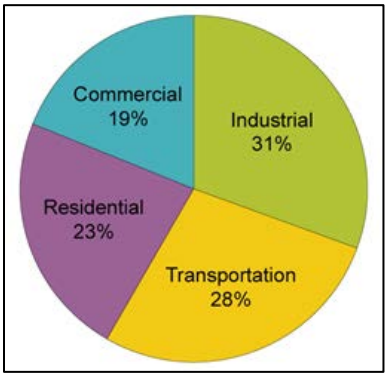

Figure 1. Share of energy consumed by major sectors of the economy, 2010

Along with clean and efficient delivery of energy to homes and businesses, transportation is a major consumer of energy and presents an even greater challenge in converting to more sustainable sources (Figure 1). The integration of electric vehicles (EV) into the SG will allow for the accountability of all major energy consumers in the energy life-cycle [8]. Like the SG, EV is a term commonly used in a wide array of contexts and often with diverging definitions. There are several types of EV generally classified based on varying reliance of electric and conventional internal combustion engine (ICE) power (Figure 2) [9]:

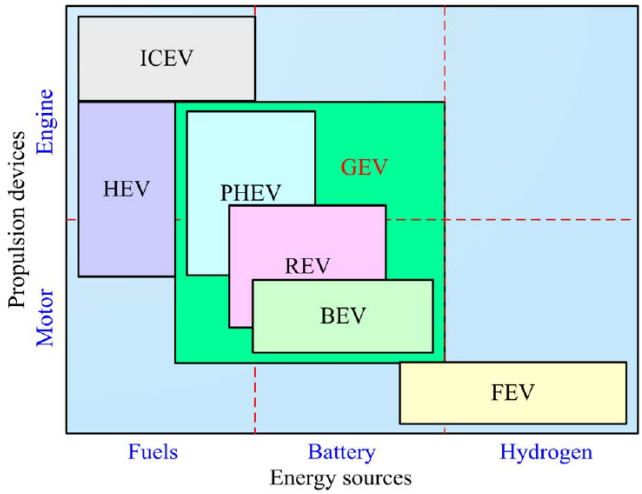

Figure 2. Classification of electric vehicle (EV) types

- Hybrid electric vehicle (HEV) – including mild, plug-in (PHEV) and range-extended (REV)
- Battery electric vehicle (BEV)

PHEV, REV, and BEV can be directly fed by electric power from the grid and are, therefore, grouped as grid electric vehicles (GEV). In this investigation, BEVs will be studied as the most complete method to fully electrify the transportation sector and cut reliance on unsustainable fossil fuels.

The average personal vehicle in the United States (US) is on the road only 4-5% of the time, sitting idle in homes, garages, or parking lots the rest of the day [10, 11]. With the automobile market trending slowly but steadily towards greater electrification, first through HEVs, then PHEVs and eventually BEVs, the resulting emergence of wide-spread energy storage capacity will have to play a pro-active role to service the future

electrical grid [11]. As already shown, transportation consumes just as much energy as the other three major sectors (residential, commercial, and industrial) all of which are predominantly supplied by the existing electric grid. Shifting the entire automobile demand onto the grid will require nothing short of a revolution to avoid potential economic and environmental catastrophe.

One of these revolutionary concepts is vehicle-to-grid (V2G), the idea of the grid having access to the vast emerging supply of energy storage space in BEVs. Hence BEVs can act not only as energy consumers but as a real energy storage medium for the network [11]. In addition to the ability to charge the BEV battery pack (grid-to-vehicle, G2V), the grid can draw from the BEV battery pack to power electrical appliances in the building (V2G). Adding BEVs and V2G to energy systems allows integration of much higher levels of RE production [12].

Hence, the BEV is not just a means used for transportation but it is a real energy storage system, accumulating surplus energy produced and giving it back to the grid at times of greatest demand [11]. V2G thus increases flexibility for the grid to better utilize intermittent RES, matching consumption and generation by discharging and charging at different times depending on market conditions [10]. Smart homes, parking lots, and public charge stations can all provide the means by which the BEV obtains or feeds energy back to the grid [13]. To summarize, the main objectives of V2G ancillary services are [10, 13, 14]:

- RES integration
- Load shifting through peak shaving and valley filling
- Reserve power supply (spinning reserves)
- Reactive power support
- Power quality maintenance through voltage and frequency regulation

In addition, vehicle-to-home (V2H) and vehicle-to-vehicle (V2V) options are defined to more precisely distinguish between different types of bidirectional energy flow [13]. V2H is the idea of charging and

discharging directly to a local home or community microgrid, without necessarily selling back to the broader utility grid. Similarly with V2V, BEVs can transfer and distribute energy through the local grid, usually by means of a controller called an aggregator. An aggregator is a control device which collects all information about a group of BEVs, grid status and executes V2V operation – it is a means by which BEVs interact with each other.

1.2. Smart energy markets - dynamic pricing and prosumer communities

For a long time, the cost of generation has varied a great deal from hour to hour; however, customers usually do not see this variability reflected in their bills [15]. As a result, there is little motivation to restrict demand at peak hours and shift load to off-peak hours [16]. Thus, dynamic pricing is a popular new solution that is discussed widely in economic research, taking advantage of modern ICT [16-18]. Schemes based on dynamic pricing are an incentive for consumers to adjust demand in response to price signals with costs varying depending on period of use and system stress [19]. Of the possible tariffing systems, real-time (RT) pricing that fully reflects operational costs would carry the highest incentives, reducing demand or shifting consumption to an off-peak period. Hence, generators and suppliers can better manage periods of tension and peak demand thanks to dynamic tariffing, as well as various demand response technologies [16].

The type of energy user who both consumes and generates energy is called the “prosumer”. Generally, prosumers produce solar and/or wind power while consuming and/or storing it for future use. Moreover, they can share excess energy generation with possible buyers including the national grid, private retailers, and other consumers. Furthermore, prosumers can retain a portion of energy in smart storage systems (e.g., battery pack in a BEV) for future use or consent to share by varying his/her own preferences. Hence, the prosumer is empowered to choose the most profitable energy trading method, either through direct selling (negotiating price per kWh) or through an auction market. One method proposed is to connect a group of prosumers, collaborating in energy auctioning, to form a “virtual power plant” (VPP) that is managed to interact and negotiate with other utility participants. Building on this idea is the “virtual community” established by combining prosumers of similar interests and behaviors, instead of geographical location [11, 20].

This SG energy sharing involves different technical infrastructures such as RES systems, smart metering, smart sensors and actuators, and ICT [20]. The smart meter is an advanced energy meter that measures energy consumption and provides added information to the utility company including voltage, phase angle, and frequency. Benefits include efficient power system control and monitoring, operational decisions to minimize outages and losses, energy cost allocation, fault analysis, demand control, and power quality analysis. Present meters are designed for centralized generation, control, transmission and distribution (T&D), and unidirectional power flow that are not sufficient for intermittent decentralized RES without compromising grid stability [21]. Mass load-shifting can be achieved in a system that allows intelligent agents to be inserted both at the grid and household level. Intelligent optimization must include new degrees of freedom offered by breakthroughs in technology controlling flows of electricity [15]. It has been estimated the effective use of new phasors and sensors could cut cost of transmission lines for RES in half [22].

The progress of ICT has been rapid and holds great potential in providing solutions for optimizing all elements of the power value chain - generation, transmission and reserve power, distribution, and metering [15, 18, 23]. Computational intelligence will play a crucial role in maximizing PHEV and BEV technology, both at the grid level and within the cars themselves [15]. Information is necessary for energy players and regulators to provide a competitive market and allow SGs to achieve optimal efficiency. The fitting of sensors to the grid will also mean data on failures will be more readily available and that the grid can be reorganized after an outage [16].

1.3. SG experimentation

Much of the research already discussed is based on macro-economic data and theoretical models. Individual SG concepts (i.e., V2G, load shifting, smart storage) have also been studied separately without combining into a complete system. It is understandably difficult to physically simulate macro-economic concepts, such as dynamic pricing and wholesale energy markets, but individual microgrid features can be constructed within a reasonable research time and budget. For instance, bidirectional V2G requires simply a BEV battery pack and two transmission lines to the grid. RES load shifting can be tested with an intermittent source (e.g., wind or

solar) and storage device (e.g., battery pack or pumped hydro). Smart metering can be simulated for an individual home or business with the integration of a local sensor network and control system. These are the main SG concepts that will be the focus of this investigation.

In specific, Chapter 2 presents the concept of a small-scale model and the design of the physical grid and control program coding. Chapter 3 presents the fully constructed grid, experimentation conducted with the control program and results from the experimentation. Chapter 4 discusses the results, how they relate to other SG investigations and ideas, and recommendations for future SSSG iterations. Chapter 5 reviews the investigation and draws conclusions.

2. Small-Scale Smart Grid (SSSG) Planning and Design

This chapter follows the design process from proposal and specification requirements to a conceptual design of the physical smart electrical grid. The data acquisition system is also presented with the LabVIEW program design including coding.

2.1. SSSG Proposition

Having established the motives and ideas behind the SG concept, the next logical step is to build one and turn virtual ideas into actual solutions. Many SG ideas have been discussed and modeled several times without testing real components or piecing together full assemblies. While backed up by perfectly reasonable assumptions, these results are purely theoretical and, therefore, limited in value. In an idea as advanced and complex as the SG, unpredictable issues will arise when several apparently simple solutions (e.g., bidirectional V2G, V2H, advanced ICT, reserve power, etc.) are combined. The experience of a real SG model can provide invaluable understanding of a relatively new and unknown concept.

Ideally, a large-scale model provides the most accurate simulation; however, the cost and size of a full-scale SG is of macro-economic proportion and beyond the scope of an investigation of this manner. Downsizing to a small-scale smart grid (SSSG) not only cuts cost and complexity immensely, it is far more practical for experimentation. The logistics of data acquisition and the ability to observe the arrangement in its entirety are of utmost importance in researching and developing the system. Of importance, the setup must remain dynamic to accommodate frequent progressive changes and upgrades.

Safety is also imperative and unpredictable issues are a recipe for disaster at the large-scale with amplified current and voltage magnitudes. Even with secure protection, the full-scale power flows implemented in the industry and standardized by the Society of Automotive Engineers (SAE - over 6 kW in the case of BEV charging) are extremely hazardous and cannot be perfectly isolated in a research and development project requiring continuous tinkering, updating, and maintenance [24-28].

2.2. SSSG Architecture

Conceptually, the SSSG is designed to mimic a SG as closely as possible. Renewable generation, battery storage, and bidirectional V2G are key concepts that can be downsized relatively simply. A functional model is developed displaying all components and energy flows required (Figure 3). The lower region illustrates the SSSG itself with energy flows (solid lines) while the top represents data acquisition with signal flows (dashed lines). Each device tasked to perform a certain function is paired and displayed below the specific action.

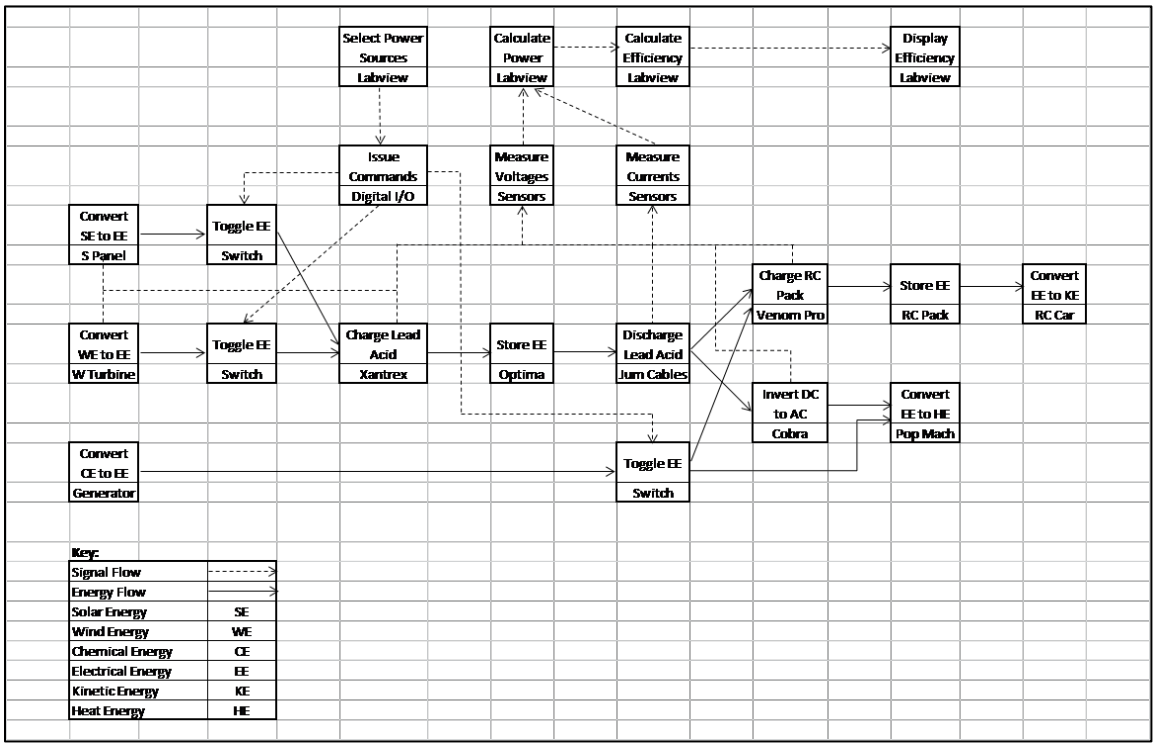

Figure 3. Functional model of SSSG concept

Specific products are then chosen to perform each of the functions above and are listed along with their specific task (Table 1). Items #1-15 are the grid itself and #16-26 are sensing and data acquisition equipment. The photovoltaic (PV) panel and wind turbine (WT) represent RE generation and the gas generator (GEN) conventional non-renewable power. The lead acid battery (LAB) represents either a grid or household smart energy bank to store excess RE, similar to those employed in previous studies [5, 29]. The BEV battery pack is represented by lithium iron phosphate cells (LIB) of the same chemistry found in modern commercially

available PHEVs [24-27]. The Xantrex Charge Controller (XCC) is employed to protect the LAB from the PV panel and WT, and prevent backflow from the LAB to the RE generators. The PV panel has a significantly higher voltage than the LAB and uncontrolled charging can seriously damage or reduce battery longevity. The XCC provides three-stage charge control (bulk, absorption and float), temperature protection, and overload and short-circuit protection [30]. A 400W modified sine wave (MSW) inverter is selected to convert direct current (DC) discharge from the LAB into alternating current (AC) power. The average peak load for the average household in the US is nearly 3kW so, for the prime energy consumer, a popcorn maker (POP) is selected as it operates at approximately 10:1 scale [39].

Table 1. Components and their functions

Item #	Part	Product	Acronym	Purpose
1	LAB Pack	Optima BlueTop D31M	LAB	Grid or household energy bank
2	Charge Controller	Xantrex C35	XCC	Protects LAB and prevents backflow to PV panel
3	Breaker Box			Safe shutdown of PV panel, WT and GEN
4	Solar Cells	50 3x6 Everbright Pretabbed DIY Kit	PV	Conversion of solar radiation into EE
5	Solar Panel Backing	Coroplast		Lightweight structure for PV panel assembly
6	Cell Adhesive	Loctite Epoxy		Attachment of PV cells to PV backing
7	Solar Panel Cover	Plexiglass		Transparent cover for protection of PV cells
8	Wind Turbine	50W Mini Turbine	WT	Conversion of wind KE into EE
9	Gas Generator	Generac 800W Generator	GEN	Conversion of gasoline CE into EE
10	Cables			Power transmission
11	Switches	Toggle Switches		Control and selection of power flows
12	Inverter	Cobra 400W Power Inverter	INV	Conversion of LAB DC discharge into AC power
13	EV Pack	12V A123 Lithium Ion	BEV/LIB	BEV energy storage
14	EV Pack Charger	Venom Pro Charger	VPC	Charges and protects LIB
15	Appliance	Waring Pro Popcorn Maker	POP	Grid or household energy consumer
16	Data Logger	NI cRIO 9073 8-Slot Real-Time Controller	CRIO	Amalgamates and transmits NI module data to PC
17	Power Supply	NI PS-15 Power Supply		Supplies and protects CRIO
18	10V Sensor	NI 9201 8-Channel 12 Bit Analog Input	NI 9201	Measures pyranometer and LEM sensor outputs
19	80mV Sensor	NI 9211 4-Channel 24 Bit Analog Input	NI 9211	Other sensor outputs (see text)
20	60V Sensor	NI 9221 8-Channel 12 Bit Analog Input	NI 9221	Measures DC voltages
21	300V Sensor	NI 9225 3-Channel Analog Input	NI 9225	Measures AC voltages
22	5A Sensor	NI 9227 4-Channel 24 Bit Analog Input	NI 9227	Measures low currents, both AC and DC
23	Digital Module	NI 9401 8-Channel Digital I/O	NI 9401	Inputs and outputs signals for grid control
24	DC Current Sensor	LEM HAIS 50-P Current Sensor	LEM	Measures high (0-50 A) DC discharge from LABs
25	Anemometer	Hall Effect Generator		Measures wind speed
26	Pyranometer	Apogee 5V Pyranometer		Measures solar irradiance

For data acquisition, the project received a 60% discount from National Instruments (NI) to employ the Compact Reconfigurable I/O (CRIO) chassis for sensor and data amalgamation. The remaining NI modules were chosen

to cover all voltage ranges for various sensors as well as direct measurement of AC and DC voltages in the grid. The NI-9227 was the only current sensing module available and could measure low AC and DC currents. The NI-9211 was chosen to read the original pyranometer, which was donated to the project but deemed too heavy and complex to integrate into the SSSG. Nonetheless, the module would eventually be employed for the current shunts, discussed in section 3.1.2. LEM hall-effect current sensors were originally chosen to measure the high current DC flows since they output an easily readable DC voltage and do not interfere with the measured discharge. They were also affordable as can be seen in Table 2.

Table 2. Planned expenditures for the SSSG

Item #	Part	Product	Quantity	Unit Price	Total
1	LAB Pack	Optima BlueTop D31M	1	$231.66	$231.66
2	Charge Controller	Xantrex C35	1	$104.00	$104.00
3	Breaker Box		1	$50.00	$50.00
4	Solar Cells	50 3x6 Everbright Pretabbed DIY Kit	1	$82.50	$82.50
5	Solar Panel Backing	Coroplast	1	$60.00	$60.00
6	Cell Adhesive	Loctite Epoxy	1	$10.00	$10.00
7	Solar Panel Cover	Plexiglass	1	$31.00	$31.00
8	Wind Turbine	50W Mini Turbine	1	$80.00	$80.00
9	Gas Generator	Generac 800W Generator	1	$300.00	$300.00
10	Cables		1	$50.00	$50.00
11	Switches	Toggle Switches	10	$3.00	$30.00
12	Inverter	Cobra 400W Power Inverter	1	$26.55	$26.55
13	EV Pack	12V A123 Lithium Ion	1	$200.00	$200.00
14	EV Pack Charger	Venom Pro Charger	1	$139.99	$139.99
15	Appliance	Waring Pro Popcorn Maker	1	$82.48	$82.48
16	Data Logger	NI cRIO 9073 8-Slot Real-Time Controller	1	$1,599.00	$1,599.00
17	Power Supply	NI PS-15 Power Supply	1	$209.00	$209.00
18	10V Sensor	NI 9201 8-Channel 12 Bit Analog Input	2	$379.00	$758.00
19	80mV Sensor	NI 9211 4-Channel 24 Bit Analog Input	1	$329.00	$329.00
20	60V Sensor	NI 9221 8-Channel 12 Bit Analog Input	2	$529.00	$1,058.00
21	300V Sensor	NI 9225 3-Channel Analog Input	2	$1,499.00	$2,998.00
22	5A Sensor	NI 9227 4-Channel 24 Bit Analog Input	1	$1,065.00	$1,065.00
23	Digital Module	NI 9401 8-Channel Digital I/O	1	$269.00	$269.00
24	DC Current Sensor	LEM HAIS 50-P Current Sensor	3	$25.30	$75.90
25	Anemometer	Hall Effect Generator	1	$115.00	$115.00
26	Pyranometer	Apogee 5V Pyranometer	1	$235.00	$235.00
	Smart Grid			15%	$1,478.18
	Data Acquisition			85%	$8,710.90
	Energy Infrastructure Total				***$10,189.08***

Following the choice of the components, a cost projection can be made including an estimate for all sensors, wiring, and switches (Table 2). It can be seen sensing and data acquisition equipment take up 85% of total expenditure, dwarfing the cost of the grid itself. This is chiefly because the CRIO, voltage, I/O module and weather sensors are not downsized on the small-scale so at least $6,000, or 70%, of data acquisition expenditures are equal to large-scale. However current sensing expense, already significant on the small-scale, would be inflated considering the NI-9227 is inadequate for most large-scale nodes. It must be reiterated this budget was an original proposal based on retail prices of the components in Table 1 and intuitive guesstimates of other expenses such as cables and switches. As will be shown in the next section, continuous adjustments were made during the iterative design process.

A more detailed design is conceived with a sketch mapping the expected layout of the SSSG (Figure 4). The components are organized into shelved compartments in a mobile cart. The portability of the SSSG is important for the sake of conducting outdoor RE testing and for transportation to demonstration events, such as the EPA P3 contest (the original funding for this project). This initial sketch already demonstrates some of the complexities involved with SG bidirectional power flow. Connections to and from one component cannot be limited to adjacent components. For instance, powering the household appliance (popcorn maker - POP) directly from the grid requires an extra line, not shown, to avoid the inefficiencies of the smart charger, EV pack and inverter. Also not shown, the smart charger cannot be powered directly from the LAB. It must be connected via the inverter in the top compartment to receive AC energy. As it turned out, three inverters were required to handle all the DC-AC energy flows and are discussed in detail later.

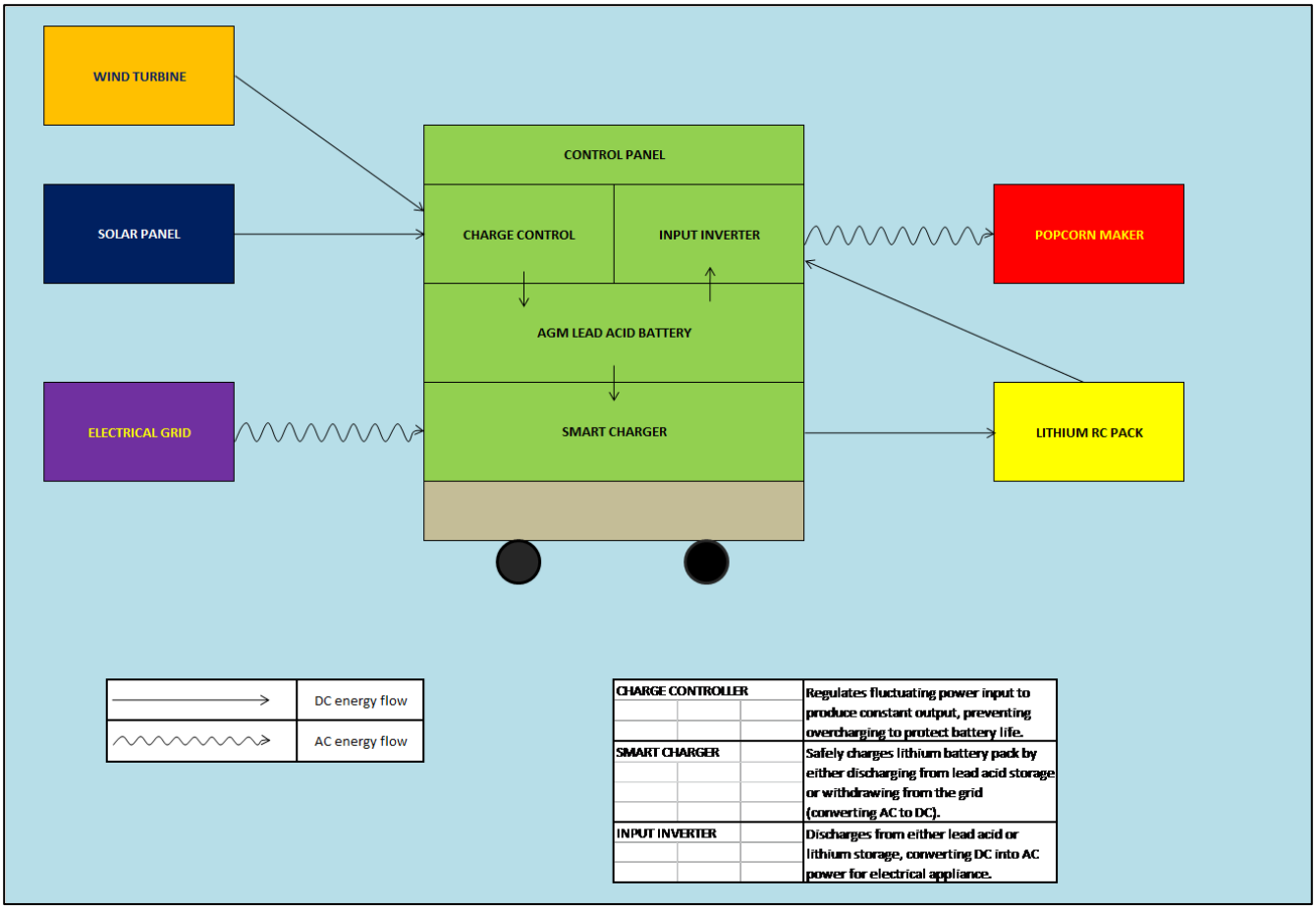

Figure 4. Diagram of SSSG cart

In order to monitor and analyze the SSSG, a network of sensors is installed to measure electrical current and voltage at various nodes. These readings are used to calculate power using Ohm's Law (in Equation 1) and efficiencies of each component (Equation 2):

$$P = I * V \tag{1}$$

$$\eta_C = \frac{P_{C,out}}{P_{C,in}} \tag{2}$$

where P is power, I is current, V is voltage, and η_C component efficiency with the subscript *out* indicating power out of the device and the subscript *in* indicating power into the device.

A National Instruments (NI) CompactRIO (CRIO) provides power for each sensor and transmits signals to the computer for processing. A program is designed in LabVIEW (LV) that will handle the sensor data, displaying

grid activity to the user mid-experiment and saving the results for post-experimental analysis.

2.3. LV Programming

LV programs and functions are called virtual instruments (VI) because their appearance and operation imitate physical instruments [31]. Each VI contains three main components – the front panel window, the block diagram (the programming code) and the icon/connector pane (for a VI to be used in another VI). The front panel of the SSSG program is a wiring diagram displaying the full structure of the SSSG (Figure 5). The idea is to present grid status to the user as clearly as possible within one window. Each block represents a device with its connections to other components including energy flows displayed in color-coded form. Clicking on a block brings up detailed information for that particular device in the form of charts covering current, voltage, power, and efficiency over time (Figure 6). The data itself is stored in memory and saved to an NI technical data management solution (TDMS) file, which is later converted to standard spreadsheet form, specified by the user at the start of the program [32].

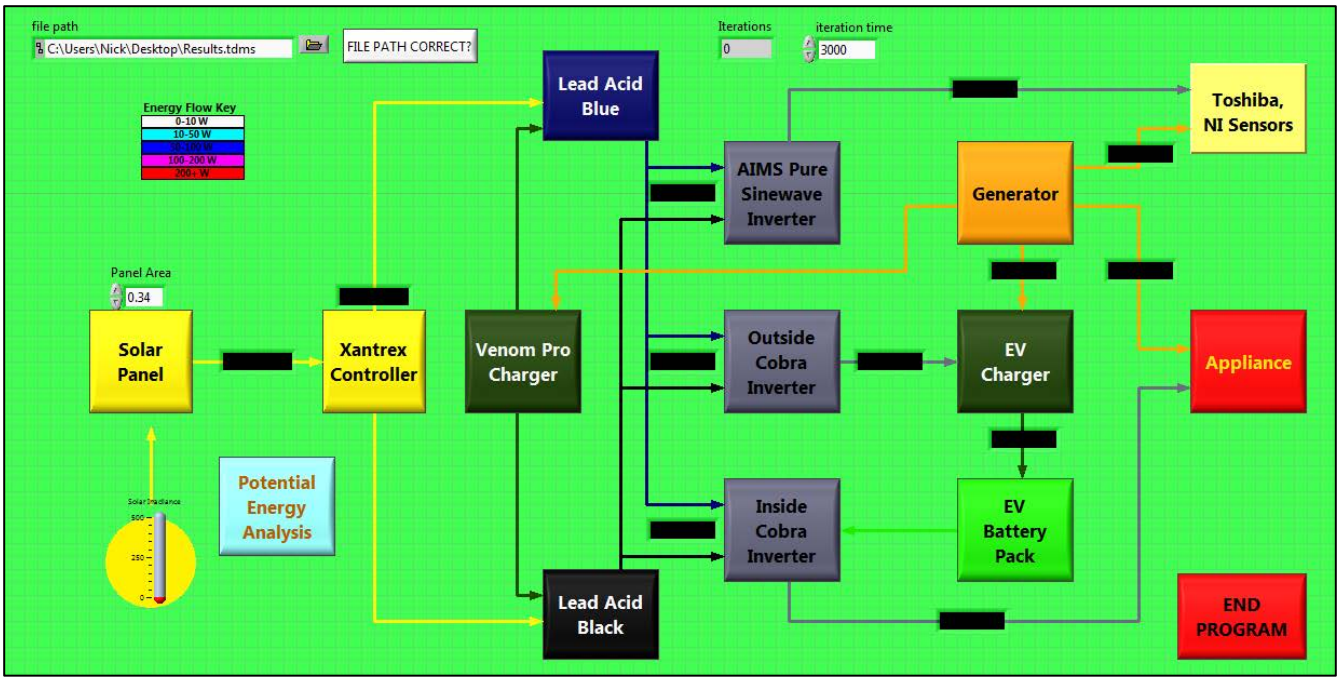

Figure 5. Screenshot of front panel of the SSSG

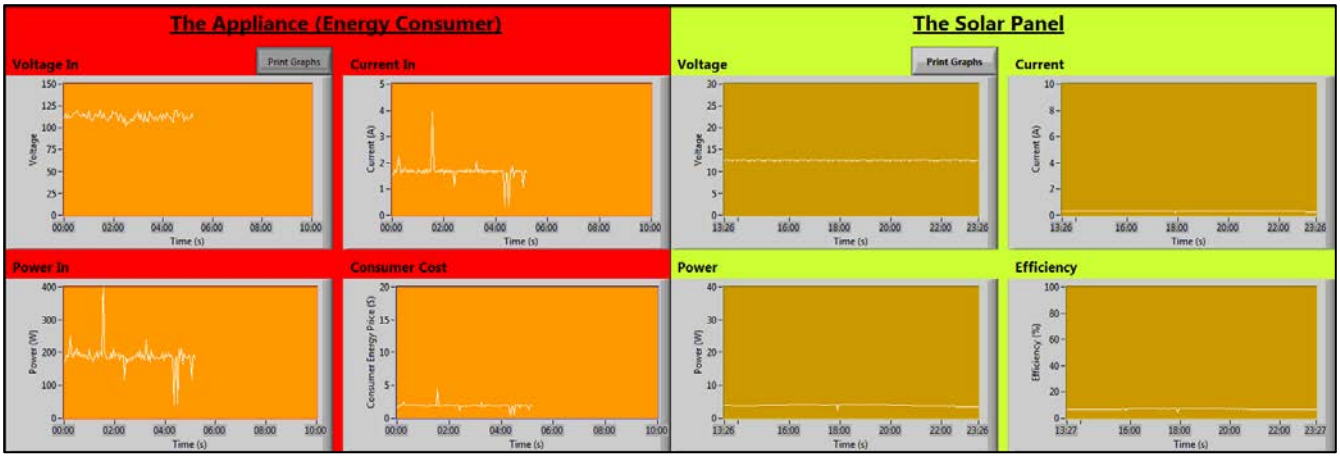

Figure 6. Screenshot of PV panel and appliance (POP) sub-VIs

The VI hierarchy embedded within the SSSG program demonstrates the overall organization of the program by representing each VI with its icon and links to its sub-VIs (Figure 7). The VIs linked to the CRIO are not shown but can be seen in the bottom left corner of the while loop in *MainFlowChartDisplay.vi* code in Figure 8. The following paragraphs describe the function of each of these VIs in more detail.

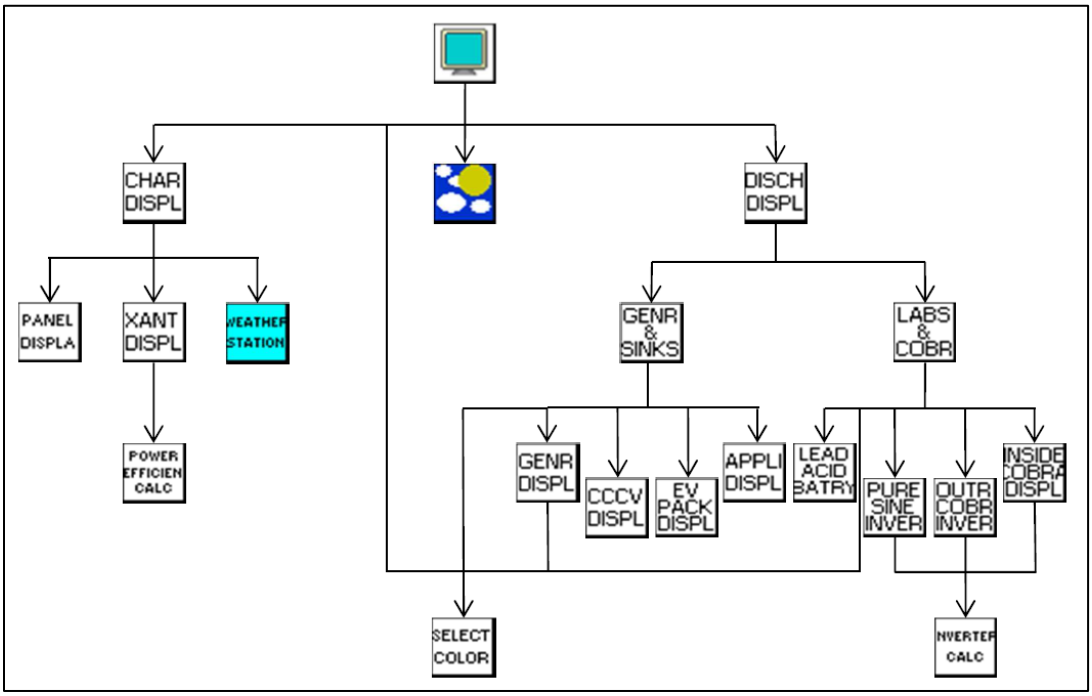

Figure 7. LV program code hierarchy indicating links between VIs

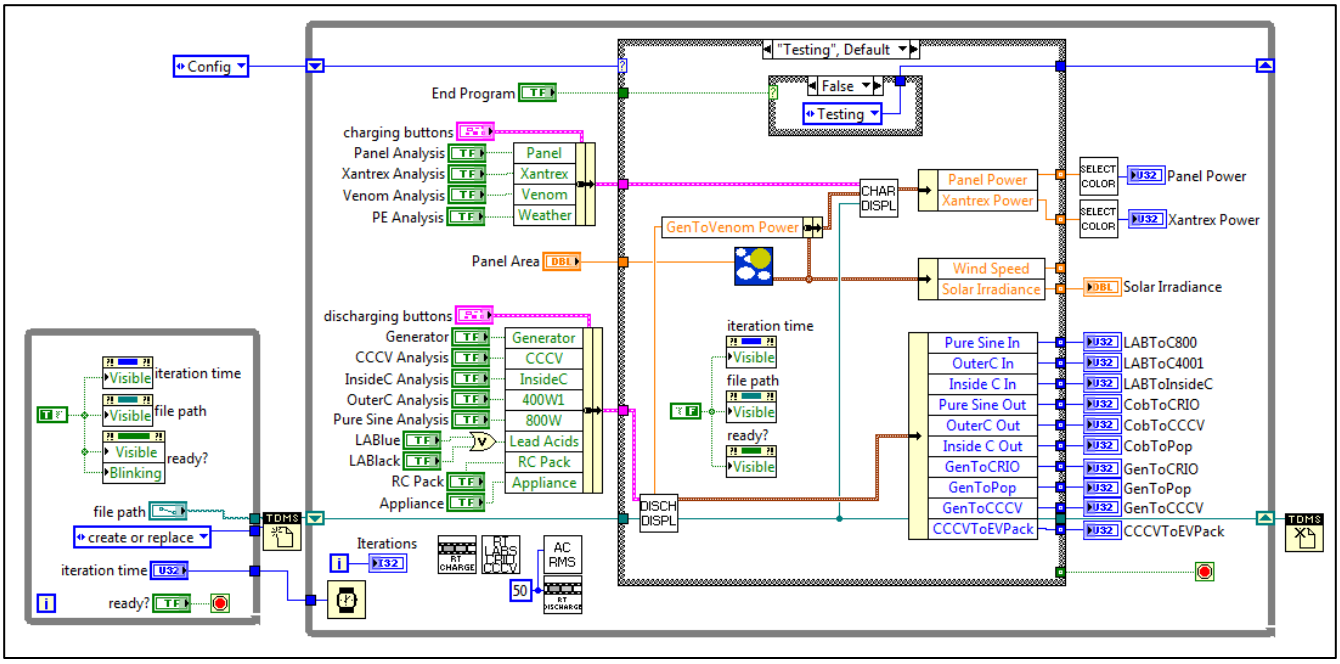

Figure 8. MainFlowChartDisplay.vi code

The main VI *MainFlowChartDisplay.vi* consists of a while loop with a set iteration delay controlling the frequency of data collection, including updating all pushbuttons and displays (Figure 8). The iteration delay is set by default to 3000 milliseconds (top center of Figure 5 under "Iteration Time"), but this can be adjusted according to the particular experiment. Within the while loop is a case structure consisting of the three phases of the program – initiation, testing, and termination. The core of the program is the testing or data collection phase. The boolean controllers aligned on the left of the case structure represent the pushbuttons on the front panel and are linked to two sub-VIs – *ChargingDisplays.vi* and *DischargingDisplays.vi* - organized to output data from various parts of the SSSG. A *WeatherReadings.vi* takes user input of solar panel area and pyranometer readings and outputs maximum available solar energy.

The *ChargingDisplays.vi* uses sensor readings taken from nodes on the energy generation side of the SSSG and outputs solar irradiance, PV panel output, and XCC data (Figure 9). The "Display Controls" are user inputs from the front panel and "Data Inputs" are effectively outputs from *WeatherReadings.vi*. Four further sub-VIs output raw voltage and current sensor readings, and power and efficiency values for PV panel and XCC. These are collected into an array called Solar that are logged to the TDMS file and output by *ChargingDisplays.vi*. A

function called *PowerEffCalc.vi* is employed by *PanelDisplay.vi*, *XantrexDisplay.vi*, and *TurbineDisplay.vi* to compute power output and efficiency of each device.

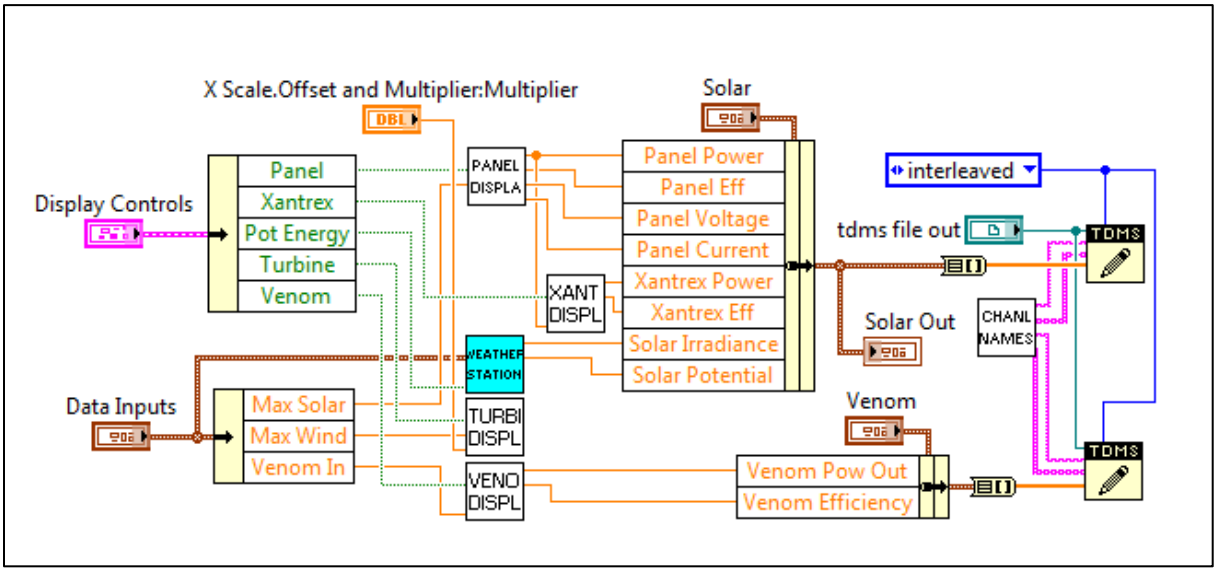

Figure 9. ChargingDisplays.vi code

Similarly, *DischargingDisplays.vi* deals with readings from nodes on the energy consumption side of the SSSG and outputs inverter, BEV, and POP data (Figure 10). "Select Display" is the array of boolean inputs from the user controlled pushbuttons on the front panel. The two sub-VIs in the middle contain the component-specific

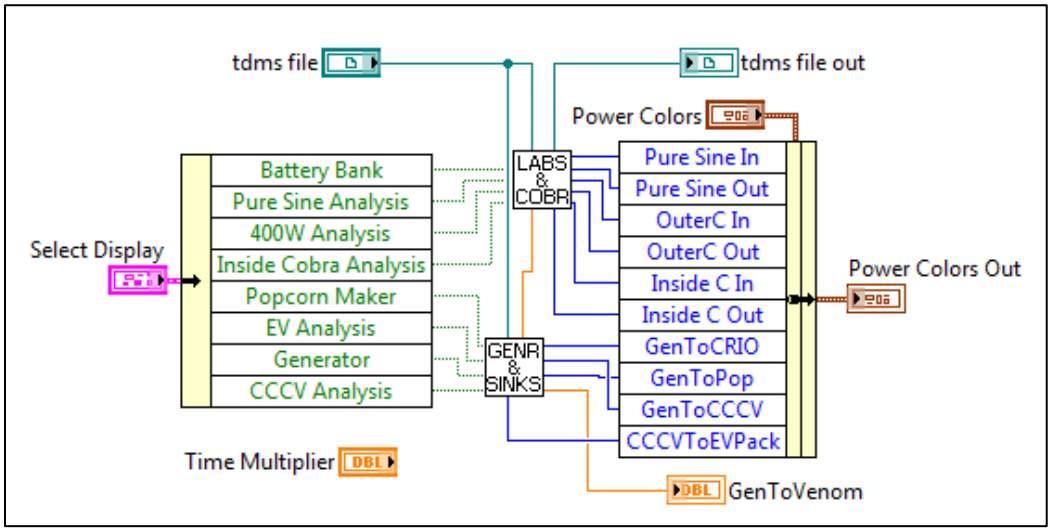

Figure 10. DischargingDisplays.vi code

sub-VIs (see Figure 10) and output an array of colors to be displayed on the front panel at the various nodes.

Lead acid batteries and Cobras.vi handles the lead-acid batteries (LABs) and each of the inverters, outputting data to the TDMS file and the color-coded power flows for each front panel node (Figure 11). The four sub-VIs in the middle handle the front panel sub-diagrams containing charts of current, voltage, and power for the particular component (Figure 6).

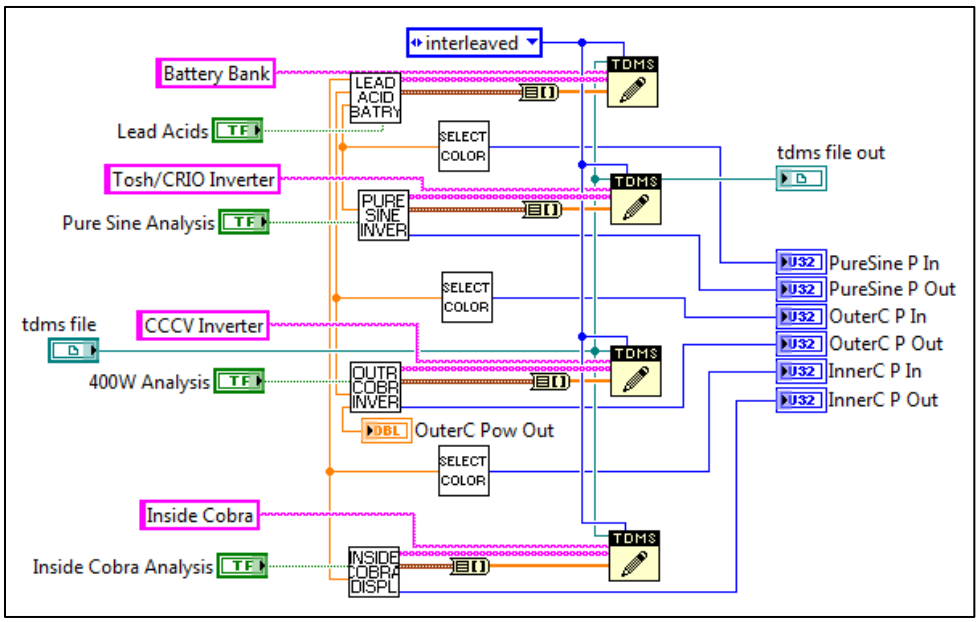

Figure 11. LABs and Cobras.vi code

Similarly, *Gen and Sinks.vi* handles POP, constant-current constant-voltage (CCCV) charger, and lithium-ion battery (LIB) outputs (Figure 12). *SelectColor.vi* generates the color to be displayed on the front panel based on power flow magnitude between devices - employed in several VIs on both the charging and discharging side (Figure 13). As can be seen top left of the front panel under “Energy Flow Key” (Figure 5), the color-coding scheme is white 0-10W, light blue 10-50W, blue 50-100W, purple 100-200W, and red >200W. An earlier version of the program displayed numerical values on the front panel; however, the color-coded approach was deemed more helpful to quickly reassure the user that the SSSG was operating correctly. If a more precise reading is desired mid-experiment, the user can click on the relevant component and read the values off the charts (Figure 6).

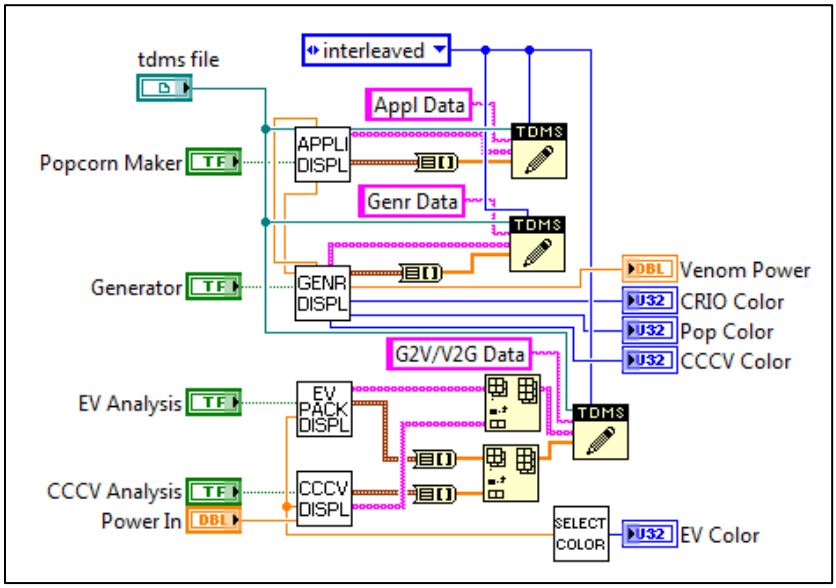

Figure 12. Gen and Sinks.vi code

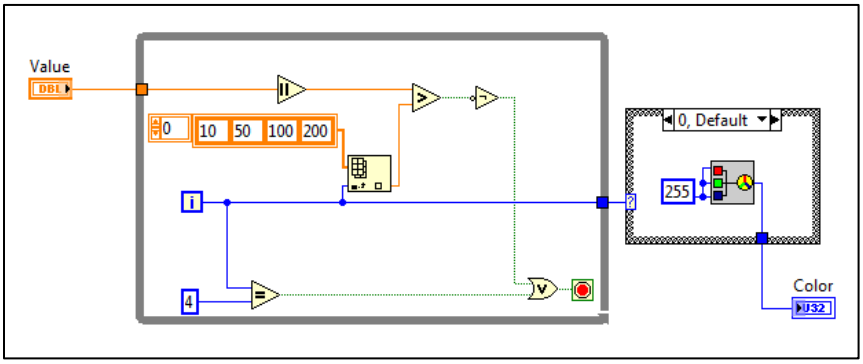

Figure 13. SelectColor.vi code

WeatherReadings.vi was originally planned to formulate and display real-time wind speed and potential power based on turbine size (Figure 14). As will be discussed later in Chapter 3, the small-scale turbine did not make the final SSSG version however the code is still included to demonstrate the full weather station concept. The Apogee SP-215 pyranometer outputs a DC voltage proportional to solar irradiance in the range of 0-4.4 VDC. This is connected to a channel in the NI9201 sensor that can be read by LV. The voltage reading is multiplied by the calibration factor 250 in order to obtain solar irradiance and then by panel area for maximum available solar power.

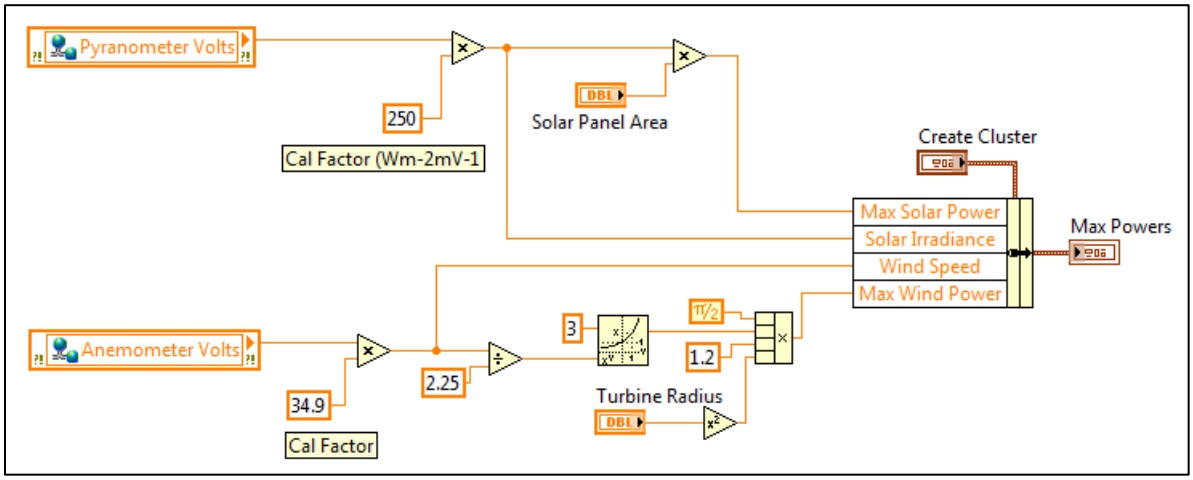

Figure 14. WeatherReadings.vi code

Not shown in the VI hierarchy (Figure 7) are the four VIs receiving data from the CRIO. Two of these are *AC Voltages.vi* (Figure 15) and *Discharging Readings RT.vi* bottom left of the while loop in *MainFlowChartDisplay.vi* (Figure 8). These sub-VIs process the AC signals from voltage sensors and convert them into root mean square (RMS) values before assigning them to global variables for the rest of the program to use (Equation 3):

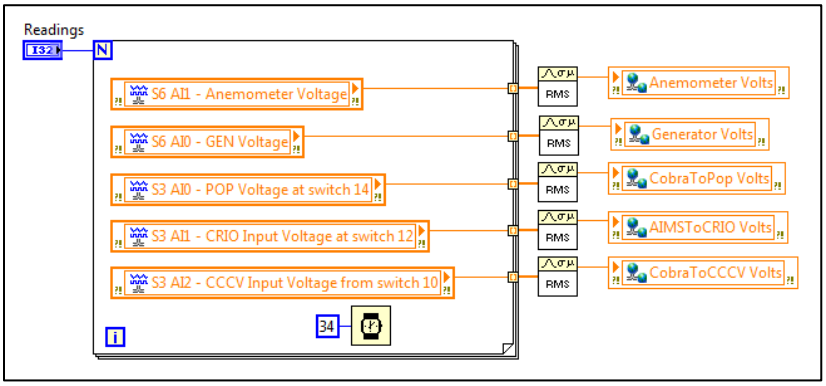

Figure 15. AC Voltages.vi code

$$V_{rms} = \sum_{i=1}^{n} \frac{|V_i|}{n} \qquad (3)$$

where V_i is a single voltage reading and n the total number of readings. The value "50" feeding into these VIs indicates each RMS calculation uses 50 raw readings to determine the value for each RMS global variable. This can be increased for greater accuracy as long as the frequency of raw data collection is fast enough to permit the

number of values in one while loop iteration.

The other two VIs *Charging Phase Readings RT.vi* (Figure 16) and *Other Readings RT.vi* take the raw DC signals and assign them to global variables without manipulation.

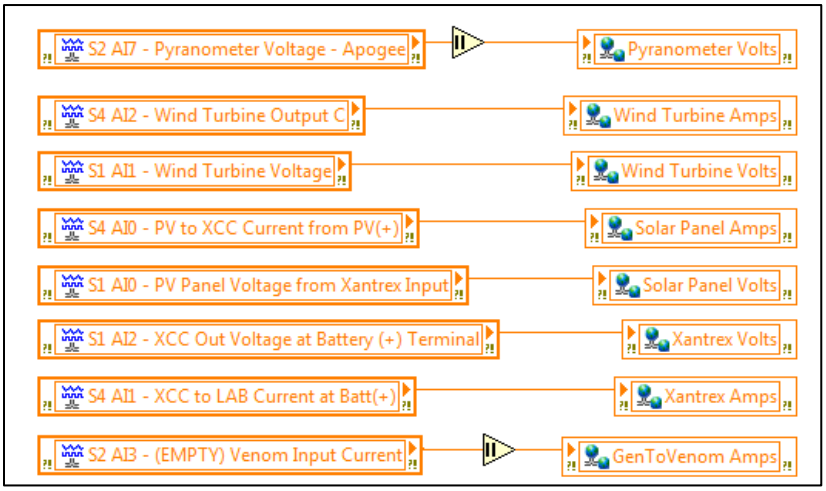

Figure 16. Charging Phase Readings RT.vi code

3. SSSG Results - Construction and Experiments

The final SSSG fully assembled on the in-house built cart presented at the EPA P3 competition in Washington DC is indicated in Figure 17. This chapter will first review the final expenditure decisions, describing the choice of components and assembly process, and then report the experiments conducted including how the results relate to other SG research.

Figure 17. Full SSSG cart assembly presented at EPA P3 competition in Washington DC

3.1 Construction results including amendments from initial design

The final budget in Table 3 effectively summarizes the changes that were made from the original plan (Table 2). It should be noted that the information provided in this table relates strictly to materials and component expenditures and does not include tools or labor. Several specific tools were purchased for this project; however, these are considered long-term research investments shared with other projects and, therefore, not exclusively part of the SSSG. Labor hours are difficult to designate to specific parts of the SSSG; hence, an accurate

reflection was not possible. For instance, many labor hours were spent working on parts omitted in the final design and many more on finding and fixing simple wiring issues. This discussion will focus on component costs that can be more definitively presented.

Table 3. Final expenditures

Item #	Part	Product	Quantity	Unit Price	Total
1	LAB Pack	Optima BlueTop D31M	2	$231.66	$463.32
2	LAB Charger	Venom Pro Charger	1	$139.99	$139.99
3	Charge Controller	Xantrex C35	1	$104.00	$104.00
4	Solar Panel	HQRP Mono-crystalline Solar Panel	1	$60.00	$60.00
5	Gas Generator	Generac 800W Generator	1	$300.00	$300.00
6	Gas	Gallon 87 Octane	2	$2.65	$5.30
7	Cables	various	1	$173.00	$173.00
8	Connectors	various	1	$290.00	$290.00
9	Toggle Switches	SPDT and DPDT Toggle Switches	10	$3.00	$30.00
10	Other Accessories	Solder, Tape, Clamps, Labels	1	$316.00	$316.00
11	400W Inverter	Cobra 400W Power Inverter	1	$26.55	$26.55
12	800W Inverter	Cobra 800W Power Inverter	1	$45.00	$45.00
13	Pure Sine Inverter	AIMS 600W Pure Sine Wave Inverter	1	$160.00	$160.00
14	EV Pack	A123 $LiFePO_4$ 26650 3.2V 2.5Ah cell	4	$17.80	$71.20
15	BMS (for EV pack)	Elithion Lithiumate Pro	1	$755.00	$755.00
16	Cell Boards		1	$120.00	$120.00
17	Appliance	Waring Pro Popcorn Maker	1	$82.48	$82.48
18	Data Logger	NI cRIO 9073 8-Slot Real-Time Controller	1	$1,599.00	$1,599.00
19	Ethernet Cable	Yello 5ft	1	$14.00	$14.00
20	Power Supply	NI PS-15 Power Supply	1	$209.00	$209.00
21	10V Sensor	NI 9201 8-Channel 12 Bit Analog Input	2	$379.00	$758.00
22	80mV Sensor	NI 9211 4-Channel 24 Bit Analog Input	1	$329.00	$329.00
23	60V Sensor	NI 9221 8-Channel 12 Bit Analog Input	2	$529.00	$1,058.00
24	300V Sensor	NI 9225 3-Channel Analog Input	2	$1,499.00	$2,998.00
25	5A Sensor	NI 9227 4-Channel 24 Bit Analog Input	1	$1,065.00	$1,065.00
26	Digital Module	NI 9401 8-Channel Digital I/O	1	$269.00	$269.00
27	AC Current Sensor	Hawkeye Hall Effect Current Transducer	4	$46.00	$184.00
28	DC Current Sensor	EMPRO HA50-50 base-mounted DC shunt	3	$27.43	$82.29
29	Pyranometer	Apogee SP-215 Pyranometer	1	$235.00	$235.00
	Smart Grid			26%	$3,141.84
	Data Acquisition			74%	$8,800.29
	Energy Infrastructure Total				$11,942.13

3.1.1. Smart grid assembly

First and foremost, despite the successful construction of a 24 VDC PV panel using solar cells and backing that

was originally budgeted, it was deemed too large and fragile for incessant transportation and testing. Instead, solar power is implemented with an HQRP mono-crystalline 20.7 VDC 1.783 A PV panel for a total potential output of 36.9 W (Figure 18). A WT was also purchased and assembled but, regrettably, was deemed inadequate since the minimum charging voltage could not be reached on the small-scale even at relatively high wind speeds over 40 mph. For this reason, as well as the difficulty testing such an intermittent inconsistent unreliable power source, wind power was abandoned in this project. The technical complications concerned with generating power from a turbine far exceed that of a PV panel and require extensive independent investigation and experience. However, issues related to the utilization of volatile wind power in the SG are covered comprehensively in the literature and will be discussed later.

Figure 18. From left to right PV panels: (a) in-house 24VDC and (b) HQRP mono-crystalline 20.7VDC

The addition of the second advanced glass mat (AGM) LAB enabled simultaneous charging and discharging for maximum grid flexibility. The original Optima Blue Top (LAB1 or Blue LA) is supplemented by an AAE Marine (LAB2 or Black LA) with nominal capacities of 75 Ah and 90 Ah, respectively [33]. The XCC was successfully integrated to control PV charge to the LAB for maximum protection. The Venom Pro Charger (VPC) manages charge into the LABs from a regular non-renewable AC source, such as the main grid (Figure 19).

Figure 19. From left to right: Optima Lead Acid Battery (BlueLAB), Xantrex C35 Charge Controller (XCC), and Venom Pro Charger (VPC)

The LIB was integrated successfully to represent BEV battery storage. Ideally, the BEV would be charged directly from the LAB and if possible straight from the PV panel. However, the sensitive chemistry of the LIB is such that it requires a battery management system (BMS) to monitor and protect the pack (Figure 20). The four 3.3 VDC cells are wired in series and must be balanced precisely in order to maintain integrity and maximize durability. This, unfortunately, leads to an inefficient transmission process of LAB to inverter, inverter to charger, charger to LIB, and LIB re-balancing by BMS. While each of these components exhibit relatively high efficiencies >90%, the cumulative losses are significant and unavoidable without a uniquely designed device that can charge directly from LAB to LIB and accurately balance the cells.

Figure 20. From left to right: A123 LiFePO$_4$ cells (LIB) and Elithion Lithiumate Pro (BMS)

The inverter capacity was significantly greater than originally considered. On top of the 400W Cobra Inverter (INV1) supplying AC power for POP (see Figure 21), an 800W Inverter (INV2) supplies CCCV with both inverters of the MSW variety. It was hoped to supply CCCV, PC and CRIO simultaneously off INV2 however it was found the PC and CRIO would not operate under MSW supply. Thus, in addition, a 600W Pure Sine Wave

(PSW) Inverter (INV3) must be employed to power the CRIO and PC (Figure 21). Considering the cost of INV3 is greater than INV1 and INV2 combined, this reiterates that the expense of sensing and data acquisition far exceeds core grid activities of the SSSG. The CRIO and personal computer (PC) can be powered directly from grid power when operated indoors; however, it is important that the entire SSSG, of which ICT is a key aspect, is self-reliant when sufficient renewable energy is available.

Figure 21. From left to right inverters: Cobra 400W (INV1), Cobra 800W (INV2) and AIMS 600W (INV3)

The Generac Gasoline Generator (GEN) was successfully integrated providing the equivalent of grid power when the SSSG is being demonstrated outdoors; indoors, a standard electrical 120 VAC grid outlet is used. The main challenges are ensuring safety with canisters of gas needing to be stored and diverting GEN exhaust emissions away from the user. Four output devices are connected – LAB, LIB, POP, and CRIO – and the current is measured into each device. The user can decide whether to operate using the GEN or plug into the conventional power grid, but not both concurrently; of note, the case makes no difference to the SSSG and it must be emphasized the only purpose of the GEN is to enable full operation outdoors where there is no access to a grid socket. However, for the sake of simplicity, GEN will refer to the non-renewable energy source of the SSSG, whether actually plugged into the generator or an indoor grid outlet.

Bidirectional V2G was more expensive and complex than expected. As already explained, a BMS was introduced to protect the LIB pack through controlled accurate balancing. A CCCV charger was selected to deliver charge to the pack and was designed to be powered by AC current. This effectively leads to the undesirable conversion of DC to AC and then AC back to DC just to transfer energy from LAB to LIB (G2V).

Discharging back to the LAB (V2G) would require setting up another input to the VPC via one of the inverters. A failsafe would also have to be installed to ensure both GEN and LIB are not supplying power simultaneously. Regrettably, this was not incorporated in the SSSG in time for this report; however, V2G is adequately covered by LIB to POP.

Time and budget limitations restrict control to a manual switchboard setup rather than a LV automated system for this early iteration of the SSSG design. Double pole double throw (DPDT) switches select XCC or INV (charging or discharging) to LAB, GEN or INV1 into POP, GEN or INV2 into CCCV, GEN or INV3 into CRIO, LAB or LIB into INV1 in situations where an available off position is important for component protection. Single pole double throw (SPDT) switches are employed to choose between XCC or VPC into LAB, and LAB1 or LAB2 grid connection. Wiring all components, sensors and switches together develops into an extremely complex exercise with items connected indirectly to each other via a current and a voltage sensor, as well as a toggle switch. This effectively made it unnecessary to cautiously pre-plan and position components on the cart for efficient wiring.

3.1.2. Data acquisition and sensors

The organization of the data acquisition slots and module channels in the CRIO are summarized in the system setup (Table 4). It can be seen the bulk of the channels are reserved for current and voltage for the sake of calculating power flows around the SSSG.

Table 4. CRIO slots and module channel assignments

Chassis cRIO 9073			
Slot 1	60V Sensor NI 9221		
	Channel 0	PV Panel Voltage	
	Channel 1	Wind Turbine Voltage	
	Channel 2	XCC Voltage	
	Channel 3		
	Channel 4	VPC Voltage	
	Channel 5	LAB1 Voltage	
	Channel 6	LAB2 Voltage	
	Channel 7	LIB Voltage	
Slot 2	10V Sensor NI 9201		
	Channel 0		
	Channel 1		
	Channel 2		
	Channel 3	Hkeye1 GEN to VPC Current	Hawkeye Current Sensors
	Channel 4	Hkeye2 CCCV Input Current	
	Channel 5	Hkeye3 POP Input Current	
	Channel 6	Hkeye4 CRIO Input Current	
	Channel 7	Pyranometer Voltage	
Slot 3	300V Sensor NI 9225		
	Channel 0	POP Voltage	
	Channel 1	CRIO Voltage	
	Channel 2	CCCV Input Voltage	
Slot 4	5A Sensor NI 9227		
	Channel 0	PV to XCC Current	
	Channel 1	XCC to LAB Current	
	Channel 2	Wind Turbine Output Current	
	Channel 3		
Slot 5	60V Sensor NI 9221		
	Channel 0		
	Channel 1		
	Channel 2		
	Channel 3	LAB to INV2 Voltage	
	Channel 4	LAB to INV3 Voltage	
	Channel 5	LAB to INV1 Voltage	
	Channel 6		
	Channel 7		
Slot 6	300V Sensor NI 9225		
	Channel 0	GEN Voltage	
	Channel 1	Anemometer	
	Channel 2		
Slot 7	80mV Sensor NI 9211		
	Channel 0	Shunt1 LAB to INV1 Current	Current Shunts
	Channel 1	Shunt2 LAB to INV3 Current	
	Channel 2	Shunt3 LAB to INV2 Current	
	Channel 3		
Slot 8			

The NI-9221 modules measure DC voltages, which usually occur in the narrow range of 12-14 VDC depending on battery (either LAB or LIB) state of charge (SOC). The NI-9201 module measures output of the Hawkeye current sensors and pyranometer, both of which will be discussed later in this section. The most expensive of the modules, the NI-9225, measures high AC voltages, namely the GEN and the outputs of the inverters. Channels are also reserved for the wind turbine and anemometer; however, as already mentioned, these are neglected in

this report.

The NI-9227 5A module measures relatively low current with strong 24-bit accuracy, but is limited to 4 channels and is the second most expensive after the NI-9225. The nodes chosen for this module are PV to XCC, XCC to LAB and WT output current. This leaves the four AC currents and three high current DC flows from either LAB into INV1, INV2, and INV3.

High current DC sensors were difficult to find, expensive, and generally lack the accuracy of low current sensors. Initially, three LEM HAIS 50-P current transducers were employed owing to their high current tolerance (50 A), low cost, and non-invasive design. These measure current through the hall-effect and output a 0-5 VDC signal to be read by the NI-9201 module for LV to convert back into the measured value [34]. However, the complexity of installation is high with an independent 22 mA 5VDC power supply required while including four pins at the bottom for powering the device and outputting the signal that was deemed incompatible with any circuit board. Ultimately, too many issues arose attempting to mount the device securely to the grid and solder solid connections to the pins so the LEM transducers were scrapped in favor of Empro HA50-50 DC shunts. The disadvantage of these is their invasive nature, effectively extracting power from the flow being measured. However, their cost is relatively low and both installation and operation are simple with the voltage output signal in the range 0-50 mVDC proportional to the 0-50 A measurable current [35]. These are connected to the NI 9211 module to be read by LV.

Four Hawkeye hall-effect current sensors are employed to measure the AC currents, outputting a proportional voltage to be read by NI-9201. LV converts these back into currents (I_{HE}) using the following relation:

$$I_{HE} = \frac{V_{HE} * C_1}{N} \qquad (4)$$

where V_{HE} is the read voltage, C_1 is the correction factor and N is the number of turns around the sensor – the wire can be wrapped several times to magnify voltage output.

Finally, the Apogee SP-215 pyranometer measures solar irradiance (*Irr*) in the range of 0-1100W m^{-2} and outputs 0-4.4 VDC to be read by module NI-9201 [36]. The correlation is linear with conversion factor C_2 equal to 250 $Wm^{-2} V^{-1}$:

$$Irr = V_{pyr} * C_2 \quad (5)$$

where V_{pyr} is the voltage read by the module. This equation is implemented in *WeatherReadings.vi* (Figure 14).

3.2 Experimental results

Several experiments were conducted to test power and efficiency of SSSG components. Various SG features were simulated and results gathered using the tools incorporated in the LV program described in Section 2.3. The analysis can be categorized into the following five tests:

1. Average power flows and efficiencies – SSSG summary
2. GEN to POP – conventional power generation and consumption
3. LAB to POP – smart storage and consumption
4. LIB to POP – V2G or V2H
5. PV to LAB – intermittent RE generation and storage

Test #1 effectively includes the averages calculated from the results of all tests, including #1-4. LV program data was recorded to TDMS files and converted to spreadsheet form for post-processing, including calculation of average power flows and efficiencies. These are presented in Figure 22 along with the approximate capacities of each LAB. The battery capacities were measured by fully charging each LAB and discharging to the POP until INV1 cuts out. Hence, with a discharge rate of around 300 W, this equates to the capacity at a C-rate of 1. These capacities are significantly lower than advertised because both units had undergone two years of continuous usage and cycling [33]. For faster charging, to conduct discharge experiments, the VPC was employed, not the PV panel. The VPC itself reports current and voltage into the battery but as a component was not perminently integrated into the grid to be measured by NI modules so no efficiency values were obtained. The capacity of the remote-control (RC) car or BEV LIB pack will be discussed in test #4. The CRIO drew 50

W most of the time (around 99% of the time) but occasionally spiked to 120 W. At these power levels, INV3 efficiency varied from 70-80%, significantly lower than INV1 and INV2While conducting tests #2-5,

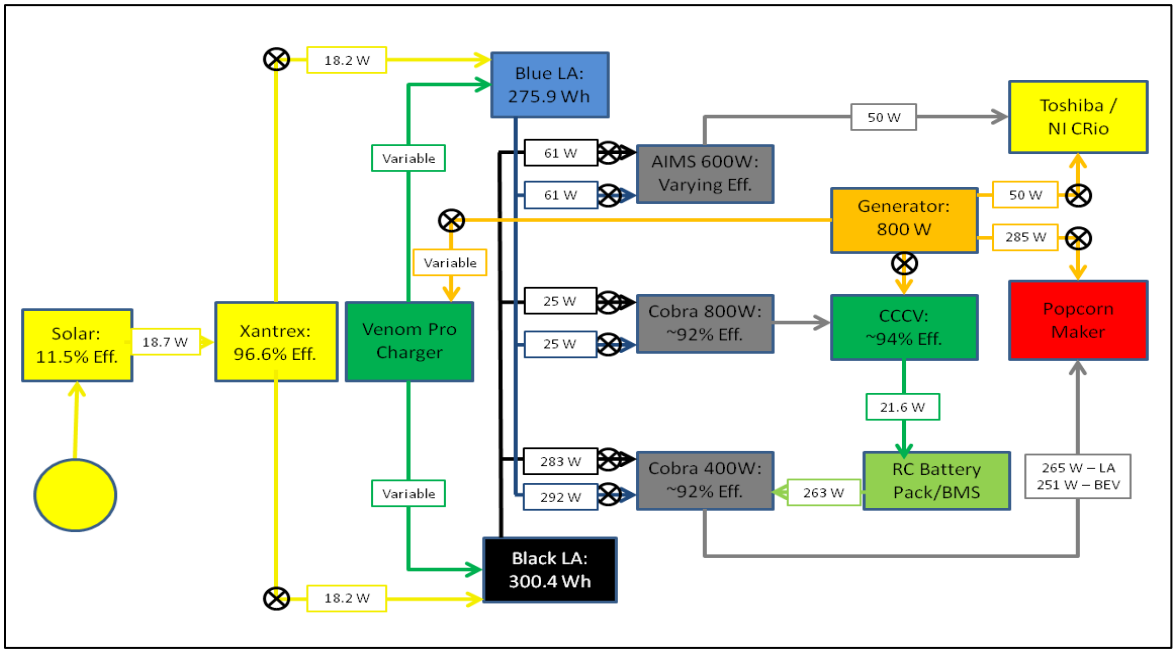

Figure 22. SG diagram with average power flows and efficiencies corresponding to test #1

With respect to test #2, the DPDT switch controlling power into the POP is selected to source GEN power. All other DPDT switches are in the off position leaving one closed node in the entire grid. The LV program is started with iteration time set to the default 3000 ms (ie sensor readings taken once every three seconds) and the POP turned on 10 iterations (30 seconds) into the program. For each cycle, the drum (or popper) is fully loaded with kernels and left until nearly the full batch of popcorn has been released. The POP is turned off, reloaded with kernels and switched back on – the process of refilling taking approximately 30-40 seconds. Data is recorded to the TDMS file and, following the experiment, converted to spreadsheet form for processing.

Figure 23 displays power flow from GEN to POP over four rounds, each representing the time and energy taken to cook one full batch of popcorn. The first cycle is the longest, due to the cold start, with subsequent cycles approximately equal in length. Maximum power draw of 285 W is instantly reached and maintained until the user switches off the machine. The results indicate adequate precision of the raw unfiltered readings despite

noticeable fluctuations of approximately ±60W and occasional anomalies. These are caused by noise between channels within each NI module and the limited RMS calculation procedure in LV (limited to 50 readings per calculation). However, the results can be rolled to more accurately reflect the situation with a precision of ±10W.

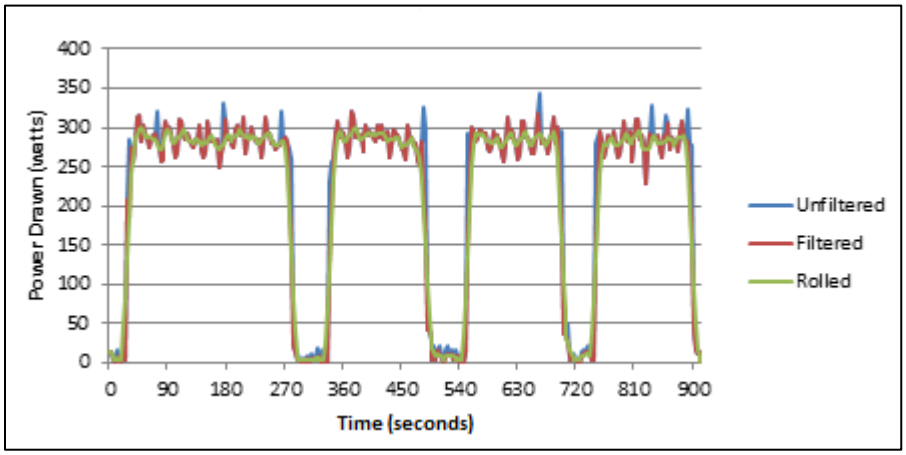

Figure 23. Power drawn by the popcorn maker over four cycles

To simulate discharge from LAB to INV to POP for test #3, the DPDT switch controlling power into the POP is selected to source INV, DPDT for INV1 is switched to source LAB (not LIB), DPDT for LAB1 is switched to INV (discharge mode) and the SPDT switch controlling LAB source is shifted to Blue LA (LAB1). All other DPDT switches are in the off position leaving LAB1 to INV1 to POP as the only closed nodes in the grid. The LV program is started with iteration time set to 3000 ms, INV1 is switched on after 20 iterations (60 seconds) and POP turned on after a further 60 iterations (180 seconds). Data is recorded to the TDMS file and, following the experiment, converted to spreadsheet form for processing.

Data at both nodes, LAB1 to INV1 and INV1 to POP, are plotted in parallel (Figure 24). Immediately noticeable is the 50 W base power drawn when INV1 is switched on but POP remains off. When POP draws the maximum 280 W power, LAB discharges 300 W to INV1 for an efficiency of 92% wasting only 20 W. INV1 operates at greatest efficiency when maximum operational power is drawn so optimal management of inverters could be a crucial aspect of economical SG management. One of the key factors in battery degradation is C-rate [14] and with a capacity of 300 Wh, a 300 W discharge corresponds to a C-rate of 1 which has little influence on

degradation [37].

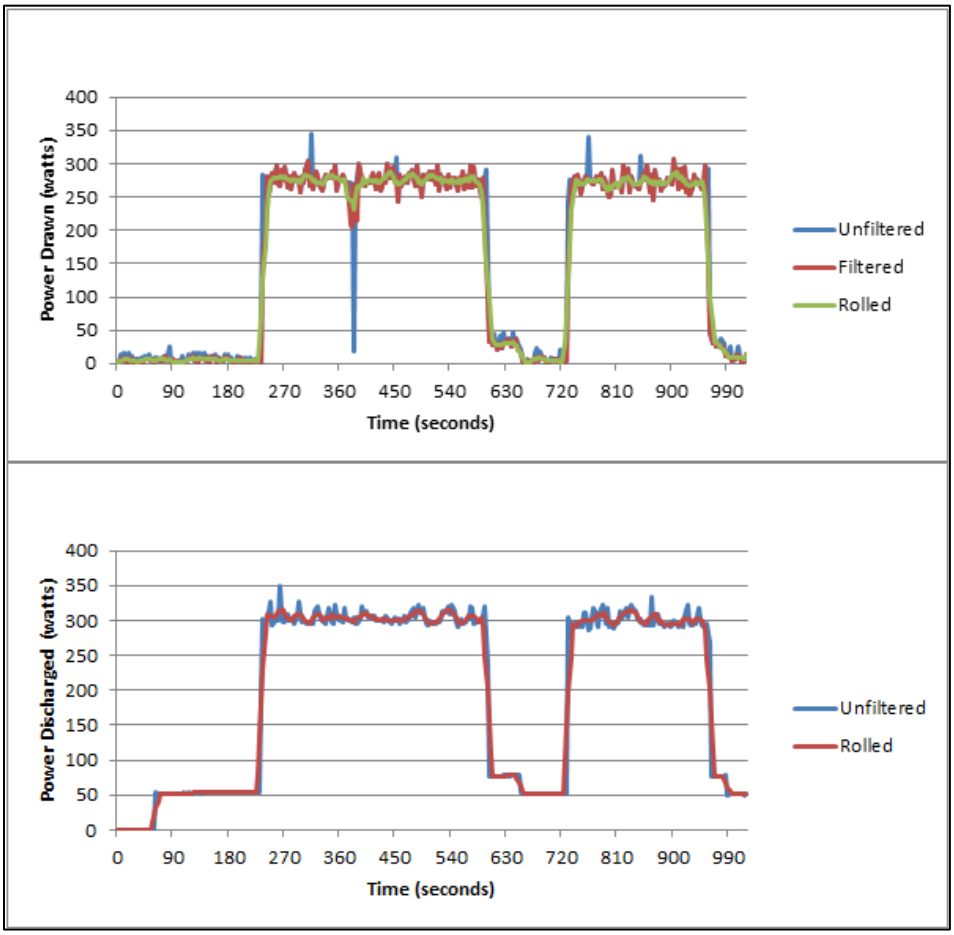

Figure 24. Power flow from LAB to POP with the top figure indicating INV1 to POP and the bottom figure demonstrating LAB1 to INV1

Test #4 simulates discharging the BEV (LIB) pack to INV1 to POP. The DPDT switch controlling power into the POP remains in the INV position, DPDT for LAB1 remains in INV position, DPDT for INV1 is switched from LAB to LIB and all other DPDT switches are in the off position. LV iteration time is set to 3000 ms and both INV1 and POP switched on after 2 iterations.

Test #4 is the equivalent of V2G or V2H with the appliance powered directly from the BEV battery (Figure 25). The total area under the curve is the energy discharged from the pack, the red shaded area is power delivered to the POP, and the grey area power lost through INV1. Most noticeable is the incomplete second cycle which cuts

out as the pack is drained exposing the limited capacity. Using trapezoidal rule to integrate the power curve, the total LIB capacity at the given discharge rate is 50 Wh. Hence, a 270W discharge equates to a C-rate of 5.4, which explains the limited capacity.

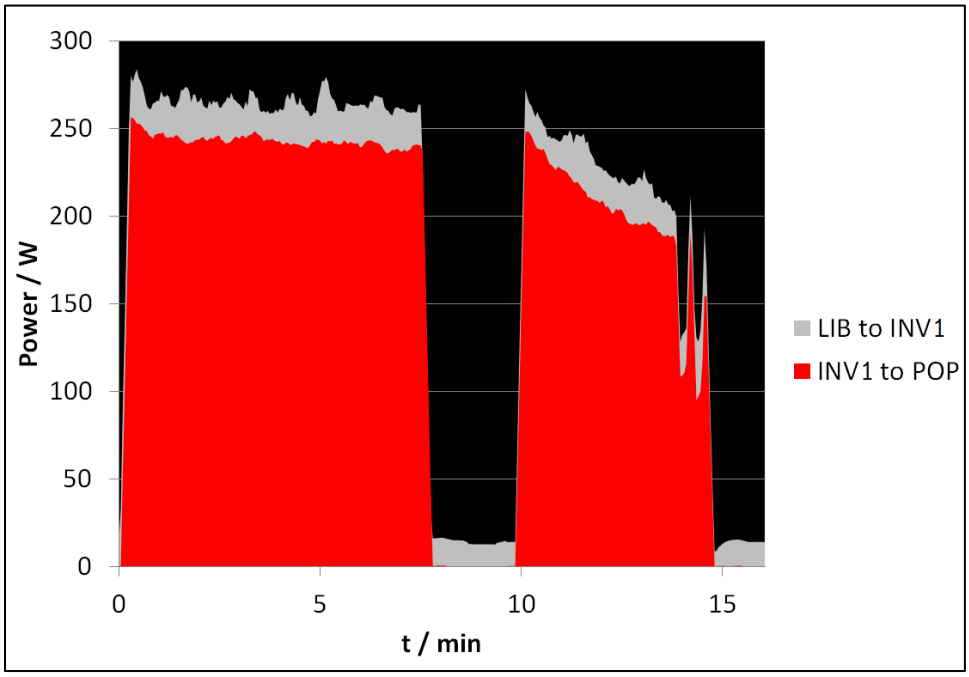

Figure 25. Power flow from LIB to INV1 to POP

To demonstrate charging from PV to XCC to LAB, test #5 readings are taken in two conditions – clear and overcast. SPDT switch controlling LAB connection is set to LAB1 and DPDT switch for LAB1 is set to XCC (charging mode). The maximum number of iterations LV can save to TDMS in a single run is around 500 so iteration time is set to 6000 ms to ensure readings can be taken for 30 minutes.

In clear sunny conditions, the charge is stable with small ±0.2W deviations from the mean and minor efficiency losses over the XCC (Figure 26). In changing overcast conditions, PV output fluctuates almost as acutely as solar power (Figure 27). In both figures, the green shaded area represents energy received by the LAB and the yellow area energy lost through the XCC. The efficiency of the XCC does not change with charge magnitude and remains constant even in the case of rapidly fluctuating input.

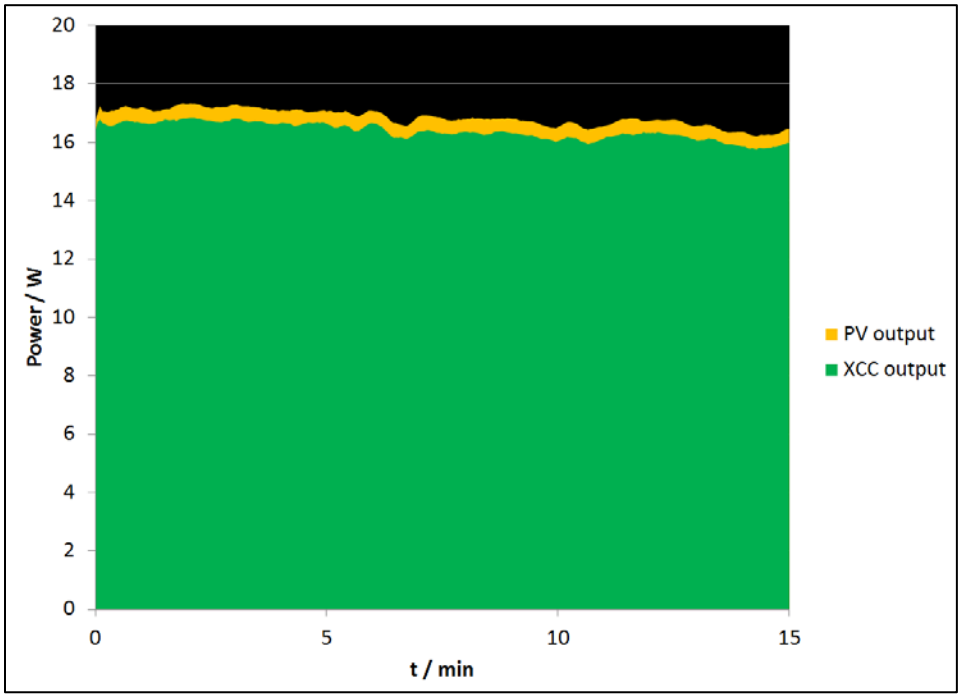

Figure 26. Power flow from PV to XCC to LAB in clear conditions

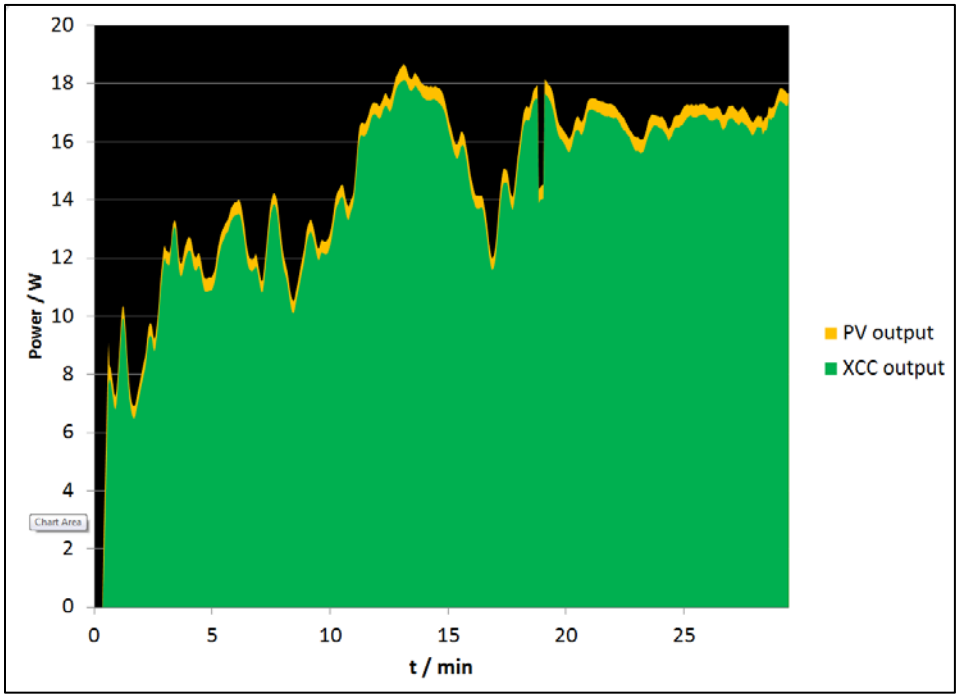

Figure 27. Power flow from PV to XCC to LAB in changing overcast conditions

PV panel efficiency is estimated by measuring solar irradiance and multiplying by panel area to obtain the total potential solar energy. It was found to peak at 11.5% (Figure 22) during times of strong sunlight, in-line with

typical commercial cell efficiency under normal operating conditions, but could drop as low as 8.5% in the late evening [38]. Efficiency can be maximized by varying the angle of the panel throughout the day to ensure it faces directly towards the solar radiation. The XCC operated at 96-98% efficiency, irrespective of PV power output. With a LAB capacity of 300 Wh, an 18.1 W charge equates to around 16 hours of charging time.

4. Discussion of SSSG Results

This chapter will explain experimental results in terms of how they can be projected onto large-scale SG. The first section relates established SG concepts with the experiments from this investigation and the second section explores other SG ideas and whether they can be simulated on the SSSG.

4.1 Projecting SSSG results to full-size SG

This section discusses the 5 tests from Chapter 3 and their results, and how they are applicable to full-size SG issues.

4.1.1 Test #1 discussion

With respect to test #1 involving the power flows and efficiencies given in Figure 22, it will be difficult to project these figures for a full-size SG. The average peak load for the average household in the US is nearly 3kW but this varies dramatically depending on size, location, and time of year [39]. Hence, the 300W POP approximately represents peak load at a scale of 1:10. Keeping with this scale, the 0.34 m² 18.7W PV panel represents a 3.4 m² 187 W panel and the LABs a 6 kWh battery bank. One study estimates 5 kW PV panel size for average detached homes in the US, 3 kW for average attached homes, and 2 kW for other homes [40]. So for a consistent 1:10 scale, it could be reasonable to expand to 3-7 m^2 (200-500W) PV size for the SSSG. Another study employs 5 m^2 PV panels with 30 kWh battery capacity for a simulated full-size DC smart house system [5]. Large-scale BEV projections are discussed in more detail as follows but immediately noticeable from Figure 22 is the mismatch between charge and discharge power – most studies take G2V and V2G power magnitudes as equal.

Figure 22 emphasizes the complexity and difficulty of simulating simple SG concepts. In specific, the role of energy conversion (AC/DC) adds significantly to efficiency losses, especially charging LIB from LAB. The CCCV and BMS limit charge into the LIB to 25 W to ensure cells are balanced. Fortunately the 800 W MSW INV2 maintains adequate efficiency at low power operation unlike its 400 W counterpart INV1. The CCCV

appears to operate at around 94% efficiency whether converting MSW AC from INV2 or PSW AC from GEN into DC. However net efficiency from LAB to LIB is 86% and PV to LAB is 96.6% so even neglecting LAB cycling losses, overall efficiency from PV to LIB is 83.5% compared with 94% from GEN to LIB. This is an expected issue RE generation and storage faces for full-size SGs. Future SSSG research should consider designing a device that converts LAB discharge straight into LIB charge, without conversion to AC. With a BMS protecting the pack, it may be possible to keep the entire LAB-LIB node in DC with a DC-DC converter. Further testing has to investigate target output voltages which cause least damage to the LIB.

4.1.2 Test #2 discussion

In regards to test #2, GEN to POP in Figure 23, conventional power generation is simulated as a reference or base scenario for other experimental results to be compared. As already discussed, this is for measuring accuracy and precision of the sensors and data acquisition methods employed. Unfiltered raw data fluctuates dramatically and produces several anomalous spikes so for practical analysis the results have to be rolled into local averages.

Even in the most simple single node test, readings are volatile and care has to be taken to reduce noise. In "Smart Grid Automation" [41], the solution is to attach Ferrite beads to magnetically absorb unwanted electrical interference (Figure 28). They can be simply snapped over wires with high noise, significantly cleaning up the signal. It is highly recommended to employ these in future SSSG iterations since noise can cause reading error over ±10%.

Figure 28. Ferrite bead tested on the SSSG

To summarize test #2 results, the first batch takes approximately 250 seconds cooking at 285 W which equals 20

Wh energy consumption. Subsequent cycles are 150 seconds at 285 W equating to 12 Wh – so an extra 8 Wh are needed to operate from a cold start. These values will be used as a comparison for other POP experiments.

4.1.3 Test #3 discussion

For test #3, LAB to POP via INV1 (Figure 24), this experiment demonstrates the discharging side of the smart energy storage system. Generally, this is employed in-house in smart buildings but also can represent a microgrid storage and distribution point in an intelligent energy network [11]. The first cycle, the cold start, takes 350 seconds at 275 W, 10W lower than GEN to POP, equating to 27 Wh, 7 Wh greater than GEN to POP. This exposes the limitation of MSW compared with PSW as the AC motor in the POP does not efficiently mix the kernels, costing an extra 35% in energy compared with GEN to POP first batch. Similarly the subsequent cycle takes 250 seconds at 275 W for 19 Wh consumption, 60% more than the GEN to POP equivalent. So it can be concluded the efficiency losses supplying a POP through MSW are unsatisfactory.

Many electrical loads draw around 20% more power with the MSW than using a PSW inverter; hence, the raw efficiency values in Figure 22 do not tell the whole story [42]. Greater deployment of PSW may be necessary despite the expense, for adequate efficiency and to reduce long-term wear on sensitive appliances [43]. In addition, certain sensitive components, such as the CRIO and PC, do not run at all off MSW, which is the reason the PSW inverter was employed. The obvious problem with using nothing but PSW inverters is the expense – four times greater than MSW (Table 3). Also shown in Figure 24 is the 50W base load drawn by the inverter even when the appliance is switched off. It is also generally the case that inverters perform at greatest efficiency when running closer to maximum operational capacity [42]. On the large-scale, with rapidly fluctuating power consumption, this may be an even greater issue and would require smart management of possibly several inverters for a single in-house storage unit. This could certainly be investigated on the SSSG by employing several 10-100W loads instead of one 300W load.

The unexpected 50 W base load from LAB1 to INV1 when the POP is switched off is a significant waste and emphasizes the need for smart inverter management. The predicted 85-90% efficiency from the device manual

[44] appears marginally pessimistic when the POP drew 275 W. On the other hand, even 85-90% may be optimistic for appliances more sensitive to MSW such as microwaves, drills, clocks or speed motors [43]. Some of these have to draw more than usual due to the poor quality of MSW, not accounted for in the INV efficiency calculation. Top of the line PSW inverters can convert DC to AC as efficiently as MSW but more importantly they deliver high quality power allowing optimal operation of household appliances. However the expense is significant, as mentioned previously, and even an inverter like the AIMS (INV3) needs to run close to maximum operational power for maximum efficiency. Hence the design and development of a smart inverter system, possibly as part of the smart metering system, will have to be investigated to optimize DC-AC conversion efficiency.

4.1.4 Test #4 discussion

Expanding to test #4, LIB to POP shown in Figure 25, this V2G experimentation is one of the core purposes of the SSSG. The first POP cycle takes 7.5 minutes (450 seconds) with a noticeably declining power draw of average 245 W for a total energy consumption of 30 Wh. This is 10% more energy than the equivalent LAB to POP cycle and 50% greater than GEN to POP. Average INV1 efficiency is 92%, same as LAB to POP, but power drawn is 30 W lower. Hence even the fully charged LIB cannot discharge at high enough power to supply POP with 275 W and this causes even greater efficiency losses on top of the MSW issues discussed previously.

The result of this investigation highlights the greatest hindrance towards wider penetration of BEVs - the limitation of modern battery technology (Table 5). On the other hand, modern BEVs are equipped with 20 kWh Li-ion packs and 6 kW chargers [24-27]. If the discharge magnitude for V2G/V2H services is assumed equal, this would equate to a C-rate of 0.3; much lower than 5.4 in this demonstration. To represent modern BEVs at the 1:10 SSSG scale suggested previously, a 2 kWh Li-ion pack should be employed with a 600W charger for future SSSG iterations. This should at the very least cut the extra 10% energy required to cook the first batch of popcorn since a low C-rate of 0.15 would be required to feed 300 W into the INV1.

Table 5. Common battery chemistries and their attributes

Battery Type	Energy Density		Durability	Charge/Disch
	Wh/kg	Wh/l	Cycles	Efficiency
Lithium-Ion	100-250	250-620	400-1200	80-90%
Lead-Acid	30-40	60-75	500-800	50-92%
Nickel Metal Hydride	60-120	140-300	500-1000	66%

4.1.5 Test #5 discussion

Finally test #5, the PV to LAB in Figure 26 and Figure 27, finds that approximately two days of 18.1W charging is required to fully charge a depleted 300 Wh LAB unit. This is extremely tedious for cyclic battery testing and determining charge/discharge efficiency. For a full efficiency analysis of PV to POP, it may be desirable to employ greater PV capacity in the SSSG for fast LAB charging in less than four hours, as long as C-rate is kept at a safe level – less than C/3 is recommended for LABs [33, 45]. Also noteworthy, the volatile PV output in Figure 27 does not hinder LAB charge since the XCC maintains voltage at a steady level despite variable power input. The graph also demonstrates the sustained efficiency of the XCC, even under relatively low levels of charge.

It should be noted that to maintain cyclic life and performance, state-of-charge (SOC) should be kept within a range of 25-95%, leaving 70% of total capacity usable [46]. In the DC smart house model, continuous generation and consumption kept the in-house battery within 25-75% SOC in almost all scenarios employing 5 m^2 (~ 400W) PV panels and a 30 kWh battery [5]. For this purpose, it could be useful to add a feature to the LV program which estimates battery SOC. Each cell type has a predictable pattern in terms of bulk, absorption and float stage voltages when charging and similar models for discharging. These can be incorporated into the program along with input and output power readings from NI module sensors.

Combining these last two ideas for future SSSG iterations, if a 1 kWh LAB is employed, a 200 W PV panel would charge from 25% to 95% SOC in three and a half hours – much more convenient for cyclic efficiency experimentation. Another study analyses a utility scale PV plant with battery energy storage; however, this

assumes most PV generation is immediately consumed by the grid and employs battery capacity equivalent to 38 minutes of total peak PV generation [6]. Overall, the PV and LAB setup in this SSSG investigation is more equivalent to a smart home or VPP than a utility scale PV plant but the two setups discussed in [6] could be tested in a future SSSG iteration.

4.2 Other SG developments

Several SG ideas have been discussed in the literature, some of which can be incorporated and tested in the SSSG but others are of macro-economic proportion and cannot be simulated using a simple model.

4.2.1 Other renewable and carbon-neutral power generation

Without renewable and carbon-neutral generation, the purpose of the SG and BEV concepts effectively become obsolete; hence, greater deployments of wind, solar, tidal, and hydroelectric power are essential. Nuclear, geothermal, and biomass sources can also be considered depending on the given priority, whether it is for continuous long term energy production or reduction of greenhouse gas (GHG) emissions. It is important to distinguish between RES, which are naturally replenished on a human timescale, and carbon-neutral sources (CNS), which emit no GHG. For instance, biomass and geothermal power are RES but not CNS; whereas, the reverse is true for nuclear. As a proportion of total electricity production, RES market share in the US actually fell in the period 1980-2001 from 15% to 8% but recovered in 2007-2011 to 12% thanks to a sharp recent rise in wind generation (Figure 29) [47]. CNS has flat-lined in the same period at around 25-30%, but could possibly be seeing the start of a long term rise, again thanks to greater wind penetration (Figure 30) [47]. In terms of the most sustainable sources (both CNS and RES) hydroelectric has flat-lined but wind, solar, and tidal are showing sharp rises thanks to government subsidies and research and development progress. However, for the most part, these sources remain insufficient and unprofitable without financial support. For instance, solar and wind power were subsidized by $60 billion in 2012 [48]. The SG attempts to address some of these issues, including inconsistent supply, with advanced infrastructure but this effectively becomes a chicken and egg problem. Without RES, the SG does not solve the sustainability issue and, without the SG, RES remains inefficient. Deploying both simultaneously may be premature and economically reckless if reliable technology is not

established and energy prices are not kept under control.

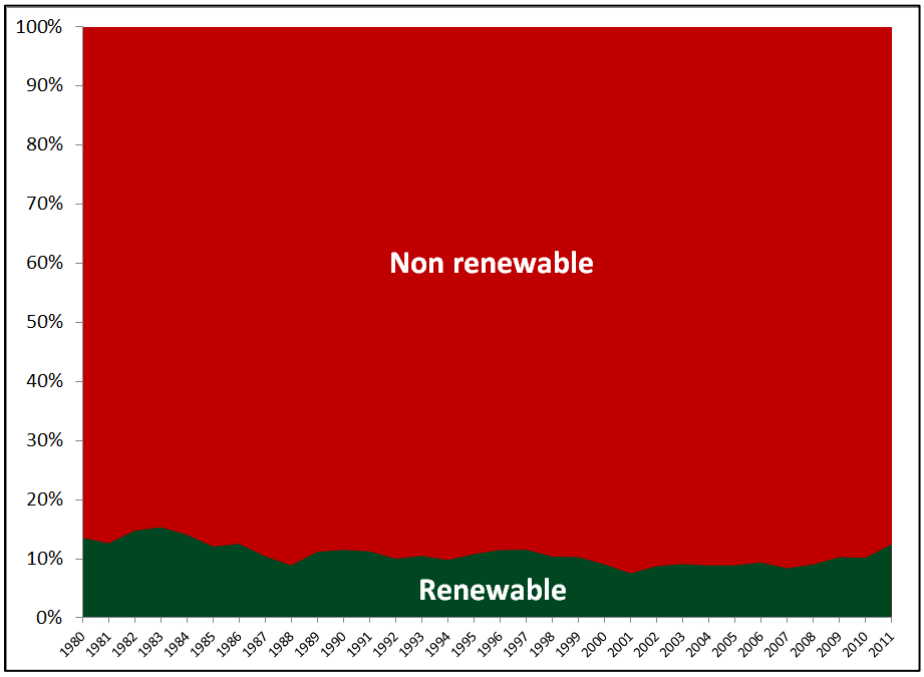

Figure 29. Renewable share of US electricity production 1980-2011

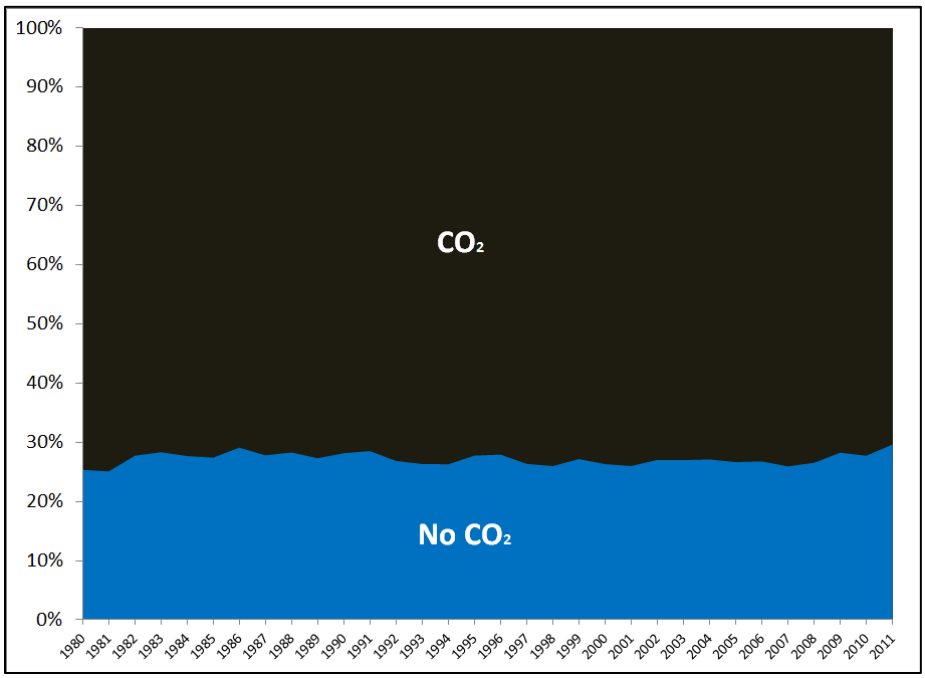

Figure 30. Carbon-neutral share of US electricity production 1980-2011

As already mentioned in Section 3.1.1, the original SSSG design attempted to incorporate wind energy (Figure 4) but the minimum voltage required to charge LAB could not be reached. However, the issues with SSSG wind turbine integration run far deeper. Modern commercial turbine requirements include [49]:

- Yaw system to keep the rotor in-line with the wind
- Gear box to generate 1000-3000 rpm demand of electric generator
- Actuators to adjust blade pitch, change angle of attack and adjust shaft power
- Advanced structural support and aerodynamic design

In addition, the intermittent unpredictable nature of wind makes it excessively laborious to incorporate into the SSSG. Although on the large-scale, policy studies have shown T&D load can be controlled by shifting charging into off-peak times with a relatively simple control algorithm [7].

Nuclear, geothermal, and tidal are also unworkable on the small-scale, for obvious reasons. Hydroelectric, on the other hand, can be accommodated if only for the purpose of SG storage. Pumped-storage hydroelectric schemes are already widely implemented to support national grid fast reserve or reactive services for sudden spikes in demand [50, 51]. With wider implementation and capacity it can also be employed for smart storage of excess renewable generation and does not comprise toxic battery chemicals or cyclic durability issues.

Pumped hydroelectric storage can be simulated on the SSSG with two large reservoirs of water and a bidirectional generator and pump assembly, such as a vane pump with DC motor (Figure 31).

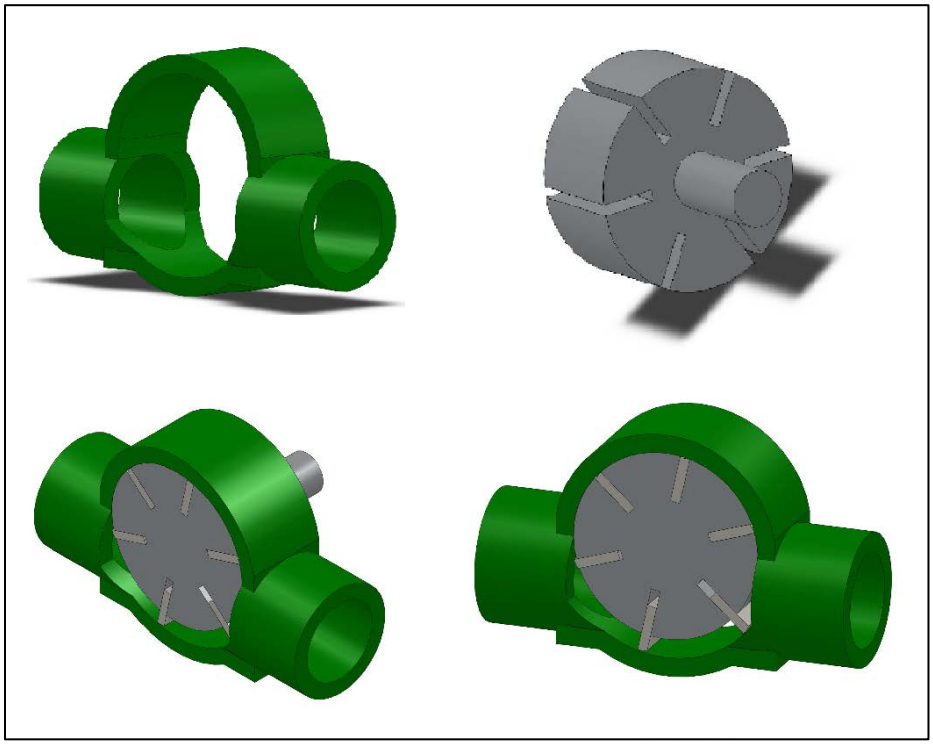

Figure 31. Hydroelectric bidirectional generator/pump design for energy storage. Clockwise from top left: housing, impeller, vane pump assembly (x2)

However, energy density is very low and representing a large-scale plant, such as the electric mountain [50], requires significant tank or upper reservoir capacity. Gravitational potential energy can be estimated as follows:

$$G.P.E = mgh \qquad (6)$$

where m is mass of water, g the gravitational constant and h vertical distance between reservoirs. Hence for, say, a 10 m^3 tank suspended 1 m above a lake or another tank, total potential energy storage is about 27 Wh – probably less taking into account pump efficiency losses. However this could be the SSSG equivalent of a grid's fast reserve service demonstrating rapid, flexible and sustainable prevention of black-outs in cases such as Figure 25 when battery storage is depleted.

4.2.2 Improved BEV technology

Energy density severely restricts the all-electric range (AER) of a BEV to around 100-120 miles [24-27]. In order to make serious in-roads into the automotive market, it has been suggested energy density must increase to ten times the current level resulting in more than a 500 mile AER [52]. However, even a tenfold improvement in

energy density will be useless unless accompanied by solid reliability in terms of cycle life, temperature, and vibration resistance. Since many cells are stacked in series in order to achieve the required voltage, battery reliability depends on the dependability of several hundred cells [13]. As could be expected, substantial resources are being invested to explore potential battery chemistries with greater specific energies [53]. Lithium-air has theoretical potential to be almost as energy dense as gasoline (Table 6) [54, 55]; however, this is based strictly on thermodynamics and there are several serious obstacles before this chemistry can become practically viable for BEVs [55].

Table 6. Theoretical and practical energy densities of various chemistries [55]

	Energy Density / Whkg $^{-1}$	
Chemistry	***Theoretical***	***Practical***
Gasoline	13,000	1,700
Li-Air	11,680	1,700
Zinc-Air	750	350
Li-S	420	370
Li-ion	250	160
Ni-MH	200-500	50
Ni-Cd	200	40
Lead-Acid	200	40

Of interest, current lithium ion technology remains adequate for modern SSSG research as it addresses the delicate issue of maintaining precise cell balance for optimal battery longevity. However, if other BEV battery technologies wished to be integrated, the SSSG could be utilized to analyze capacity, cell balancing, charge and discharge rates, and cyclic efficiency with the proposed LV additions mentioned in section 4.1.5.

To complete the SSSG setup, especially for visual and demonstration purposes, it could be beneficial to incorporate a small-scale RC BEV car. This could also aid in researching ideas discussed in the following sections; although downsizing the on-board BMS design could be difficult.

4.2.3 Bidirectional V2G infrastructure

The V2G concept explored in the experiments is entirely dependent on BEV battery capabilities and can only become a reality once the hurdles mentioned prior are overcome. Moreover, despite strong theoretical advantages – both environmental and economic [16, 56, 57] – even more issues arise. Providing V2G ancillary services introduce additional wear on BEV batteries and accelerate replacement frequency [14]. Furthermore, significant investment and regulation is required to introduce consumer-friendly bidirectional charging infrastructure, including industry standards for manufacturers to follow [10, 13]. Without central planning and control, as well as customer cooperation, grid stability is at serious risk; converse to one of the main purposes of V2G [10]. Smart metering and ICT are essential to encourage passive consumers to become active producers by selling energy back to the grid when demand is high [58].

Upgrading grid infrastructure to accommodate bidirectional power flow will be significantly expensive and take time. Each BEV must be designed with a bidirectional charger compatible with grid infrastructure. Each building, whether residential or commercial, must incorporate appropriate transmission lines and possibly storage banks for maximum local efficiency and flexibility. Since efficiency losses are proportional to transmission distance and number of conversion components (inverters, transformers, etc.), a local battery bank may be required to maximize local excess renewable generation. Hence, the LAB in this investigation could represent either external grid or in-house storage. This, however, creates an extra upfront expenditure, further reducing the economic argument for full-scale conversion.

The SSSG could be employed to experiment with more user-friendly V2G charger designs. The current SAE industry standard J1772 charger is for unidirectional purposes only so there remains a need to investigate practical bidirectional concepts [28]. Initially, a small-scale unidirectional charger, equivalent to the J1772, can be implemented as a precursor before the bidirectional charger is developed for the SSSG. This could avoid the safety issues and expense of experimenting with proposed high-voltage requirements (240-600 VAC/VDC) for full-size BEVs [10, 13].

4.2.4 BEV battery swap stations

Current battery technology does not allow charging in less than half an hour (at best), so charging stations analogous to gas stations, are not currently feasible. In this alternate strategy, depleted batteries are swapped with a fresh pack in a fully automated process, comparable to conventional refueling. This method reduces impact on distribution systems since flexible charge timing becomes possible [10]. A discharged battery can be replaced with a fully charged pack relatively rapidly in a fully standardized transaction. Further testing on proposed models is required to solve the ultimate problem of how many batteries a swap station should hold in stock and the tradeoff between responding to dynamic electricity prices and charging batteries just when they are needed [59]. While the economic research takes place, the SSSG can be employed to design and test automated battery exchange stations. Small-scale BEV packs and robotic substitution programs can be more affordably and safely researched than on the large-scale.

4.2.5 Smart homes/buildings

Both commercial and residential buildings have to play a more active role in the SG world. They are the means by which BEVs connect with the grid. However, as has been demonstrated in this investigation, the concomitant sensing and ICT networks can be an even greater expenditure than the grid itself. The initial cost of a personal PV and battery energy storage systems (BESS) is, under present market prices and technological capabilities, not recuperated through long-term savings in energy bills [5, 6]. However, a smart all-electric home with hybrid PV/solar collector (SC) system, a ground source heat pump (GSHP), and a feed-in tariff system (allowing among other things the sale of excess energy) can cut long term bills dramatically [60]. Of note, this referenced study was conducted in a sub-tropical region with greater solar potential and less central heating demand. A similar study investigated a small community of smart houses in a SG topology with the addition of wind generation and battery storage [5]. The results of the simulation are also positive but no discussion of initial infrastructure and potential maintenance costs are made.

It may be possible to simulate the DC smart house study using the SSSG at, say, 1:10 scale employing 0.5 m^2 PV panels with 3 kWh BESS capacity [5]. However the study took place in a sub-tropical region with above

average solar irradiance so 0.7-1 m^2 panel may be more appropriate. A small-scale DC GSHP could be implemented along with DC lights for energy consumers. This however may not be useful for researching US homes which entirely depend on AC power. The role of DC/AC conversion is one of the main features of the SSSG so converting to DC smart home could be too laborious. A more conventional AC smart home could be simulated with much less conversion and comparison with the DC smart home research may be useful.

4.2.6 Economic, social, and policy hurdles

Economic and environmental research has yielded positive but also cautious analysis of the SG concept. One study presents a plan for making Croatia almost entirely self-sufficient in terms of energy supply through integration of greater wind capacity, pumped hydro storage, battery storage, heat storage, heat pumps, and BEVs [56]. Another study investigates the potential of RES in Denmark and concludes 100% dependence is possible with greater deployment of smart flexible technologies, especially into the transport system [61]. Grid flexibility is a common theme in many economic studies and dynamic tariffs accommodated through greater deployment of advanced smart metering is considered one of the keys to unlocking greater investment [17]. A German investigation looks into the obstacles and options for overcoming them for wide-spread implementation of ICT, applicable in any market [62].

Despite a strong long-term economic case, the initial investment required putting in place the necessary infrastructure for ICT, bidirectional V2G, and storage is of macro-economic proportion. According to the IEA, US investment to achieve BLUE Map energy targets would amount to $5.8 trillion over 40 years [39]. However, this is to accomplish the significantly ambitious target of cutting carbon dioxide (CO_2) emissions 81% by 2050 and is considered the best case scenario, although most likely unrealistic. EPRI on the other hand estimate $340-480 billion over 20 years with a potential net benefit of $1.3-2 trillion [63]. The OECD has calculated that stabilizing and especially cutting CO_2 emissions may result in a substantial loss in GDP [39]. On the other hand, some studies show the cost of inaction would outweigh the cost of reducing CO_2 emissions over the longer term [39].

Uncertainty regarding the gains achieved by this technology and unpredictable consumer behavior make investors especially skeptical [16]. Even in a competitive energy market with several competing players, regulatory constraints and marginal costs (when one player is under constraint) may push prices out of control [16]. The “Smart Paradox” discusses the issues of effective regulation and incentives, and the importance of encouraging the right type of investments [64]. It has been shown the quality of service can often be negatively impacted by premature investment misdirected by incentive regulation.

Resistance from industry is also substantial considering how much oil and gas producers have to lose, and manufacturers are especially fearful of the risks involved in energy revolution. Oil and automobile companies allege BEVs have a net negative environmental impact because of chemical discharges from battery manufacturing facilities and disposal. This conflicts with existing lead-acid battery marketplace results and the subsequent movement towards lower toxicity lithium-based batteries [10]. However, there can be no doubt reliable affordable energy supply is indispensable in every industry of a modern developed economy.

Public perception towards the SG revolution is mixed. Despite ambitious targets for cutting carbon emissions and reliance on foreign oil [65-67], skepticism remains over the capabilities of renewable energy and the urgency of combating climate change [68-72]. Household energy prices have seen a sharp rise in European Union countries, most notably Germany, with the most ambitious environmental targets [73-75]. However, even disregarding the issue of climate change, the benefits of long term sustainable energy independence are irrefutable. Many modern international disputes and conflicts can be at least partially attributed to the issue of oil and gas trading [76-80]. The international price of oil and gas fluctuates on a daily basis and has seen a long term rise over the last 30 years, including several unpredictable spikes [81]. It is speculated the price of a barrel of oil will reach $312 in nominal terms by 2050 [39].

The SSSG can be used to design potential smart meters for consumers, providing RT market energy price, local VPP status and household consumption. The prosumer can utilize the smart meter to specify his/her preferences of what to do with excess domestic RE generation, such as energy storage in the domestic or local BESS, share

with the community (VPP), or sell to the grid. Potential algorithms and interfaces for such a device can be developed with the SSSG, either in LV or a specially programmed stand-alone device.

4.3 Future SSSG summary

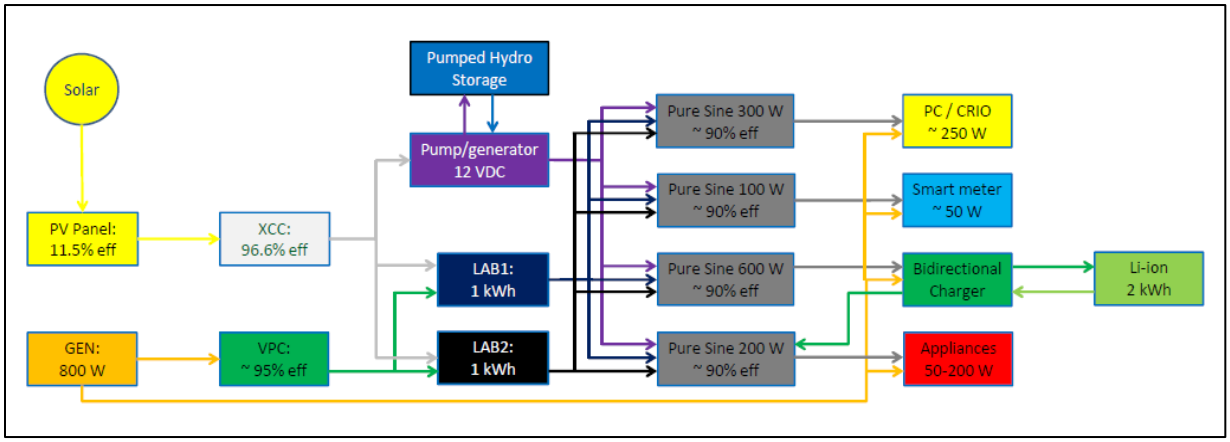

Figure 32. Future SSSG block diagram

The SSSG block diagram in Figure 22 Section 3.2 can be re-drawn to exhibit targets for future design iterations (Figure 32). Most notable is the inclusion of the previously mentioned pumped hydroelectric storage system and bidirectional charger replacing the CCCV charger. Inverters have also been converted to PSW in order to maximize efficiency and reduce wear on appliances and other energy sinks. While MSW is adequate for many devices, it is especially inconvenient for the user to have to carefully choose the correct outlet for each appliance. Since inverter efficiency peaks closer to maximum operational power, efficiency losses can be reduced by employing several smaller capacity inverters than fewer larger capacity units. However, a smart inverter management system is required to ensure idle inverters are switched off when no appliances are attached.

The LABs and BEV capacities in Figure 32 are updated to comply with proportions implemented in industry and other studies at a scale of approximately 1:10 [5, 24-27]. As well as the PC/CRIO data acquisition system, a smart meter is added to serve as a consumer friendly device to be tested in the SSSG environment. The smart meter utilizes sensor data to display power consumption and keeps the user up-to-date with RT market prices,

and LAB and BEV charge status.

5. Conclusion

The SSSG was constructed and assembled for the EPA P3 contest in Washington DC. Table 3 in Section 3.1 reveals some of the greatest expenses, including the BMS and cell boards for the lithium-ion BEV pack. This highlights the greatest hurdle facing wider market penetration of BEVs; i.e., the cost and immaturity of modern battery technology. Also striking is the significantly greater proportion of resources spent on data acquisition. Smart meters and advanced ICT have been repeatedly proposed in the literature as one of the keys to unlocking substantial energy savings [15, 17, 18, 21]. Extensive RT sensing and data acquisition is essential for the development of competitive dynamic energy pricing to encourage sustainable consumer behaviour. However, at 74% of total SSSG expenditures, the development of such advanced RT grid monitoring may be unaffordable at the large-scale. As with BEVs, data acquisition technology will require significant research and development before it can become economically viable.

The PC program designed in LV is the main tool with which the SSSG is analyzed. Power and efficiency readings are computed from raw current and voltage sensor data, as well as solar irradiance for PV efficiency. Displaying grid status to the user in a convenient manner is accomplished through a block diagram with indicators displaying power flows. Experimentation is conducted by specifying file location for the TDMS file and iteration time, with the program automatically accumulating and organizing data into manageable groups for spreasheet analysis. Future iterations of the program should adopt estimation algorithms of battery capacity, both LAB and BEV LIB, and automated control of power flow through the NI-9401 I/O module rather than employing SPDT and DPDT manual switches.

Figure 22 in Section 3.2 effectively summarizes the simulation of the SSSG. PV generation appears too low, even for a small-scale model. If the POP represents consumer load of a single home, PV panel output can be anywhere from 50-500 W based on previous studies [5, 40]. Similarly, if representing a community VPP, both generation and consumption can remain at the same proportion [5, 20]. V2G (LIB to POP) power appears more than ten times greater than G2V (LAB or GEN to LIB). This should be alleviated in future SSSG iterations by

designing and simulating a bidirectional V2G charger, similar to the SAE standard J1772 and upgrading BEV pack to 2 kWh.

Inverter management is a key factor for improving SSSG efficiency. MSW wastes up to 60% more energy cooking batches of popcorn than the PSW GEN and efficiency of the INV iteself is 92% but only when operating close to maximum. Leaving the inverter switched on without any appliance running wastes up to 50 W so household smart meter systems may have to manage inverters to minimize losses. Future SSSG iterations should be utilized to explore and design smart meters to perform such automatic management functions as well as allow prosumers to control domestic RE sources. A real small-scale BEV may also aid in smart home research and development.

A proposed block diagram for the next SSSG iteration is presented in Figure 32 Section 4.3. This SSSG approach can be exploited to cost-effectively research and develop important concepts and technologies to help secure sustainable grid operation and energy supply for the future.

References

1. Richter, B., et al., *How America can look within to achieve energy security and reduce global warming*, in *Energy Future: Think Efficiency*2008, American Physical Society. p. S1-S107.
2. Perez-Arriaga, I.J., *Regulatory Instruments for Deployment of Clean Energy Technologies.* MIT Center for Energy and Environmental Policy Research, 2009.
3. CEER, *2013 Annual Report*, 2013, Council of European Energy Regulators.
4. US-DoE. *Answering your questions about grid modernization*. 2014; Available from: http://www.energy.gov/articles/answering-your-questions-about-grid-modernization.
5. Tanaka, K., et al., *Optimal operation of DC smart house system by controllable loads based on smart grid topology.* Renewable Energy, 2012. **39**(1): p. 132-139.
6. Rudolf, V. and K.D. Papastergiou, *Financial analysis of utility scale photovoltaic plants with battery energy storage.* Energy Policy, 2013. **63**(0): p. 139-146.
7. Hennings, W., S. Mischinger, and J. Linssen, *Utilization of excess wind power in electric vehicles.* Energy Policy, 2013. **62**(0): p. 139-144.
8. US-DoE, *A Vision for the Smart Grid*, D.o. Energy, Editor 2009, Office of Electricity Delivery and Energy Reliabiltiy.
9. Chau, K.T. and C.C. Chan, *Emerging Energy-Efficient Technologies for Hybrid Electric Vehicles.* Proceedings of the IEEE, 2007. **95**(4): p. 821-835.
10. Yilmaz, M. and P.T. Krein, *Review of the Impact of Vehicle-to-Grid Technologies on Distribution Systems and Utility Interfaces.* Power Electronics, IEEE Transactions on, 2013. **28**(12): p. 5673-5689.
11. Orecchini, F. and A. Santiangeli, *Beyond smart grids - The need of intelligent energy networks for a higher global efficiency through energy vectors integration.* International Journal of Hydrogen Energy, 2011. **36**(13): p. 8126-8133.
12. Lund, H. and W. Kempton, *Integration of renewable energy into the transport and electricity sectors through V2G.* Energy Policy, 2008. **36**(9): p. 3578-3587.
13. Chunhua, L., et al., *Opportunities and Challenges of Vehicle-to-Home, Vehicle-to-Vehicle, and Vehicle-to-Grid Technologies.* Proceedings of the IEEE, 2013. **101**(11): p. 2409-2427.
14. Bishop, J.D.K., et al., *Evaluating the impact of V2G services on the degradation of batteries in PHEV and EV.* Applied Energy, 2013. **111**(0): p. 206-218.
15. Werbos, P.J., *Computational Intelligence for the Smart Grid-History, Challenges and Opportunities.* Ieee Computational Intelligence Magazine, 2011. **6**(3): p. 14-21.
16. Clastres, C., *Smart grids: Another step towards competition, energy security and climate change objectives.* 2011.
17. Faruqui, A., *Unlocking the €53billion savings from smart meters in the EU: How increasing the adoption of dynamic tariffs could make or break the EU's smart grid investment.* 2010. **38**.
18. Wissner, M., *ICT, growth and productivity in the German energy sector - On the way to a smart grid?* 2011. **19**.
19. Storelli, S. and G. Pillet, *La tarafication dynamique de l'électricité.* Bulletin SEV/VSE, 1997.
20. Rathnayaka, A.J.D., et al. *Identifying prosumer's energy sharing behaviours for forming optimal prosumer-communities*. in *Cloud and Service Computing (CSC), 2011 International Conference on*. 2011.
21. Depuru, S., L.F. Wang, and V. Devabhaktuni, *Smart meters for power grid: Challenges, issues, advantages and status.* Renewable & Sustainable Energy Reviews, 2011. **15**(6): p. 2736-2742.
22. Kreikebaum, F., D. Das, and D. Divan. *Reducing transmission investment to meet Renewable Portfolio Standards using Controlled Energy Flows*. in *Innovative Smart Grid Technologies (ISGT), 2010*. 2010.
23. Gharavi, H., *Multigate communication network for smart grid.* 2011.
24. Chevrolet. *Volt EV specs*. 2014; Available from: http://www.chevrolet.com/volt-electric-car/specs/trims.html.
25. Honda. *Fit EV*. 2014 [cited 2014; Available from: http://automobiles.honda.com/fit-ev/.
26. Tesla. *Model S features*. 2014; Available from: http://www.teslamotors.com/models/features#/.
27. Nissan. *LEAF specs*. 2014; Available from: http://www.nissanusa.com/electric-cars/leaf/versions-specs/.

28. SAE. *SAE Standards on EV charging connector approved*. 2010 [cited 2014; Available from: http://articles.sae.org/7479/.
29. Yamauchi, H., et al. *Advanced Smart House*. in *Harmonics and Quality of Power (ICHQP), 2012 IEEE 15th International Conference on*. 2012.
30. Xantrex, *C-series Multifunction DC controller: Owner's Manual*. 2010: Xantrex.
31. Instruments, N., *LabVIEW Core 1 Course Manual*. 2010.
32. *TDMS File Format Internal Structure*, in *NI web site*2012.
33. Optima. *Bluetop specs*. 2010 [cited 2010; Available from: http://www.optimabatteries.com/en-us/shop/bluetop/bluetop-group-31-dual-purpose-deep-cycle-and-starting/.
34. Farnell. *LEM Current Transducer HAIS*. 2011; Available from: http://www.farnell.com/datasheets/51649.pdf.
35. Empro. *Empro Shunts: Type HA*. 2011; Available from: http://www.emproshunts.com/product.aspx?Category=7.
36. Apogee. *Owner's Manual: Pyranometer Model SP-215*. 2012; Available from: http://www.apogeeinstruments.com/content/SP-212_215manual.pdf.
37. Serrao, L., et al. *Optimal energy management of hybrid electric vehicles including battery aging*. in *American Control Conference (ACC), 2011*. 2011.
38. Mitchell, K.W. and M.L. Tatro, *Solar cell*, in *Access Science*2014.
39. IEA, *Energy Technology Perspective: Scenarios & Strategies to 2050*, 2010, International Energy Agency.
40. Denholm, P. and R. Margolis, *Supply Curves for Rooftop Solar PV-Generated Electricity for the United States*, 2008, National Renewable Energy Laboratory.
41. Strecker, B., *Smart Grid Automation*, 2013, University of Kansas.
42. Solar-facts.com. *How much of your DC power comes out as AC power*. 2014; Available from: http://www.solar-facts.com/inverters/inverter-efficiency.php.
43. Wilson, D. *Sine Wave vs Modified Sine Wave: Which is better?* Tech Doctor, 2011.
44. Cobra, *400 Watt Power Inverter Operating Instructions*, Cobra, Editor 2010.
45. PowerStream. *SLA Battery Quick-Charging*. 2014; Available from: http://www.powerstream.com/SLA-fast-charge.htm.
46. Marano, V., et al. *Lithium-ion batteries life estimation for plug-in hybrid electric vehicles*. in *Vehicle Power and Propulsion Conference, 2009. VPPC '09. IEEE*. 2009.
47. Portal, T.D. *Browse Energy and Climate Data*. [cited 2014; Available from: http://www.tsp-data-portal.org/Breakdown-of-Electricity-Generation-by-Energy-Source#tspQvChart.
48. *World Energy Outlook 2013*, 2013, International Energy Agency.
49. Flumerfelt, R.W. and S.S. Wang, *Wind turbines*, in *AccessScience*2013.
50. electricmountain.co.uk. *Welcome to Electric Mountain*. 2014; Available from: http://www.electricmountain.co.uk/.
51. UK-National-Grid, *Fast Reserve Service Description*, in *National Grid Electricity Transmission*2013, National Grid.
52. Sperling, D. and D. Gordon, *Two Billion Cars: Driving Toward Sustainability*. 2009: Oxford University Press.
53. *Lithium/Air Battery Project (Battery 500)*. 2010; Available from: http://researcher.watson.ibm.com/researcher/view_project.php?id=3203.
54. Kopera, J. *Inside the Nickel Metal Hydride Battery*. 2004; Available from: http://www.cobasys.com/pdf/tutorial/InsideNimhBattery/inside_nimh_battery_technology.html.
55. Girishkumar, G., et al., *Lithium - Air Battery: Promise and Challenges*. Journal of Physical Chemistry Letters, 2010. **1**(14): p. 2193-2203.
56. Krajacic, G., et al., *Planning for a 100% independent energy system based on smart energy storage for integration of renewables and CO2 emissions reduction*. Applied Thermal Engineering, 2011. **31**(13): p. 2073-2083.
57. Peterson, S.B., J.F. Whitacre, and J. Apt, *The economics of using plug-in hybrid electric vehicle battery packs for grid storage*. Journal of Power Sources, 2010. **195**(8): p. 2377-2384.
58. Rathnayaka, D., et al., *Identifying Prosumer's Energy Sharing Behaviours for Forming Optimal*

Prosumer-Communities, in *International Conference on Cloud and Service Computing*2011, IEEE.
59. Worley, O. and D. Klabjan. *Optimization of battery charging and purchasing at electric vehicle battery swap stations*. in *Vehicle Power and Propulsion Conference (VPPC), 2011 IEEE*. 2011.
60. Uchida, K., et al. *Effect of energy conservation by adopted PV/SC system in subtropical regions*. in *Industrial Electronics and Applications (ICIEA), 2010 the 5th IEEE Conference on*. 2010.
61. Lund, H., *Renewable energy strategies for sustainable development.* Energy, 2007. **32**(6): p. 912-919.
62. Wissner, M., *The Smart Grid - A saucerful of secrets?* Applied Energy, 2011. **88**: p. 2509-2518.
63. EPRI, *Estimating the Costs and Benefits of the Smart Grid*, 2011, Electric Power Research Institute.
64. Marques, V., N. Bento, and P.M. Costa, *The "Smart Paradox": Stimulate the deployment of smart grids with effective regulatory instruments.* Energy, (0).
65. Obama, U.P. *Securing American Energy*. 2012; Available from: http://www.whitehouse.gov/energy/securing-american-energy#energy-menu.
66. *Reducing the UK's greenhouse gas emissions by 80% by 2050*. 2014; Available from: https://www.gov.uk/government/policies/reducing-the-uk-s-greenhouse-gas-emissions-by-80-by-2050.
67. *EU greenhouse gas emissions and targets*. 2014; Available from: http://ec.europa.eu/clima/policies/g-gas/index_en.htm.
68. Lomborg, B., *The Poverty of Renewables*, in *Project Syndicate*2014: Miami.
69. *Political leadership is lacking: Desertec founder laments lack of support*, in *Spiegel*2012.
70. *The Global Warming Policy Foundation*. 2014; Available from: http://www.thegwpf.org/.
71. Schmeller, J., *Germans grow sceptical over shift to renewables*, in *Deutsche Welle*2013.
72. *John Howard: One religion is enough*, 2013, GWPF: London.
73. Birnbaum, M., *Germany faces energy balancing act*, in *The Washington Post*2012: Berlin.
74. Faiola, A., *In Germany, going green gets expensive*, in *The Washington Post*2009: Gelsenkirchen, Germany.
75. Lomborg, B., *Germany's energy policy is expensive, harmful and short-sighted*, in *Financial Times*2014.
76. *S Sudan "will not go to war" over oil dispute*, in *Al Jazeera*2013.
77. *Oil theft in Nigeria: A murky business*, in *The Economist*2013.
78. *Ukraine crisis: EU and US impose sanctions over Crimea*, in *BBC*2014.
79. Schipani, A. and J.P. Rathbone, *Oil at the heart of Venezuela's turmoil*, in *The Financial Times*2014.
80. *Crimean crisis*. 2014; Available from: http://en.wikipedia.org/wiki/2014_Crimean_crisis.
81. US-EIA. *WTI Spot Price FOB*. 2014.